nature portfolio

https://doi.org/10.1038/s41586-021-04240-5

Supplementary information

Single-year radiocarbon dating anchors Viking Age trade cycles in time

In the format provided by the
authors and unedited

Supplementary Information

Single-year radiocarbon dating anchors Viking Age trade cycles in time

Bente Philippsen[1,2], Claus Feveile[3], Jesper Olsen[1,2] & Søren M Sindbæk[2]

[1]Aarhus AMS Centre, Department of Physics and Astronomy, Aarhus University. Ny Munkegade 120, DK-8000 Aarhus C, Denmark.
[2]Centre for Urban Network Evolutions (UrbNet), School of Culture and Society, Aarhus University. Moesgård Allé 20, DK-8270 Højbjerg, Denmark.
[3]Museum of Southwest Jutland. Tangevej 6B, DK-6760 Ribe, Denmark

Contents

List of Figures and Tables

Excavation and artefact chronology

Ribe and the Northern Emporium Excavation

Ribe, a riverine city near the Wadden Sea coast of Denmark, is one of a small group of maritime trading places or emporia that emerged along the coasts of the North Sea and the Baltic from the 600s CE onwards [28, 59-61]. Excavations since 1972 have revealed remains from intense occupation beginning c. 700 CE [62,63]. In the central settlement area, up to 2 m of stratigraphy is preserved, comprising remains of buildings, activity layers, and settlement refuse. Due to fortunate preservation, the stratigraphy remains relatively well preserved, with only moderate modern disturbances and bioturbation. The layers are rich in finds relating to a range of specialized crafts as well as non-local objects and materials that testify to active long-distance trade.

The Northern Emporium project, funded by a grant from the Carlsberg Foundation, undertook a detailed stratigraphic excavation of an area in the centre of the settlement area of early Ribe [39]. The excavation was conducted in collaboration between the Centre for Urban Network Evolutions (UrbNet) at Aarhus University and the Museum of Southwest Jutland, and took place from June 2017 to August 2018. (Finds and archival records are stored at the Museum of Southwest Jutland, file no. SJM 3 Posthustorvet). The excavation uncovered an area of c. 87 m^2 covering most of a building plot, together with parts of a street and adjacent plots. The excavation was carried out using a systematic stratigraphic protocol and high-definition documentation methods, including 3D laser scanning of all exposed surfaces, wet sieving of all excavated soil, and systematic geoarchaeological sampling of excavation units [45].

Phases and subphases

A total of 1,163 excavation units ('A' units) were separated in the course of the excavation. Some large units, which could not be subdivided based on physical observation, were separated into smaller spits or areas ('x' units). Units which could be recognized as parts of buildings or other constructions were grouped as construction units ('K' units). Most of these were located either on the most fully uncovered building plot ('plot 1') or the partially excavated plot ('plot 2'), which lies to the northeast of plot 1 on the opposite side of the central street.

The excavation units are divided into 18 main phases ('F' units), defined as contemporary units and constructions, which could be determined across the excavation area based on observed stratigraphic relations. Phase F1 is the natural subsoil, and F2 is the natural vegetation surface preceding the settlement. Phases F3–F14 comprise the stratified remains of a continuous settlement in the trading port dating between c. 700 – 900 CE, while F15–F18 are bioturbated activity layers and truncations from later activities and occupation.

Much of the volume of phases F4–F6 is made up of units A882, A590, and A440 – thick organic layers in which no pervasive stratigraphy could be discerned. The lack of stratigraphic structure presents a problem in assigning artefacts to specific phases. Some finds associated with these units cannot be assigned to one phase, but must be related jointly to phases F4–F5 and phases F5–F6. For the same reason, only small numbers of finds can be assigned specifically to the phases F4 and F6. For convenience, the diagrams in the main paper (Figure 2) assign layer A882 to phase F4 and A440 to phase F6, although they are kept separate in the detailed tables below.

In some phases, several subphases are defined for parts of the excavation area based on stratigraphic relations.

Phase F8 subdivisions: Most of phase F8 consists of a thick organic layer, A396, in which little or no stratigraphic structure could be traced. Across most of plot 1, however, it was subdivided by the ash layer A434, which enables us to separate finds from excavation units below this level (A396 X1012–15 and X1721) as phase F8a, and units above as phase F8b (A396 X942, X944–5, X950, X977, X979–80, X986, X990, X997, X999, X1003, X1010-11, and X1717).

Phase F9 subdivisions: Within plot 1, a sequence of several building episodes defines six subphases. At the bottom of the sequence, a massive ash layer (A391) and associated features (A368, A383, A385, A393, and A394) make up phase F9a. Phase F9b comprises the lowest clay floor patches and other features associated with building K21 (A379, A381–2, A384), including a brown activity or levelling layer

(A377). Phase F9c is made up of features above this layer (A355, A358, A360, A362–3, A367, A370, A376) and below the second clay floor of K21 (A352–4, A356–7), which defines phase F9d. A distinctive ash horizon (A350–1), associated with the termination of building K21, also belongs to phase F9d. Finally, a partly outdoor activity deposit (A335) and associated features (A332–3, A344–9) constitute phase F9e. Soil micromorphology studies have demonstrated that the phase F9e deposits comprise a floor layer, which was exposed to outdoor conditions and bioturbation after the temporary abandonment of the building [48]. Outside plot 1, a less detailed subdivision can be observed with a thick organic waste layer (A365) being roughly contemporary with phase F9a–d, and separate from layer A343 and A334 above, contemporary with phase F9e–f.

Phase F10 subdivisions: a building structure on plot 1, K22, can be followed through a sequence of several subphases. The phases are separated by three clay layers covering most of the building, interpreted as repair events to the house floor; each separates thin organic layers, interpreted as occupation debris. Phase F10a comprises units from the lowest clay floors and the associated occupation layers (A313, A315, A316, A317, A318, AA320, A321, A323, A326, A328, A329, A330, A331, A338). Phase F10b comprises units from the middle clay floors and the associated occupation layers (A288, A292, A293, A294, A295, A303, A319). Phase F10c comprises units from the top clay floors and the associated occupation layers (A266, A275, A276, A280, A281, A282, A283). Phase F10d constitutes a thick organic layer above the last occupation (A263 and A270), which probably represents the demolition of the building and levelling of the plot.

As the phases and subphases are compared to the artefact distribution, a number of changes are observed over the course of the approximately two centuries of activity documented by the stratified deposits. The gradual appearance and disappearance of find types across the phases and subphases confirm the division of phases.

Artefact finds

A total of 107,226 artefact finds are recorded from the excavation in addition to 939.1 kg of animal bones. The most numerous find groups are ceramics (31,089 items); glass, including raw material and workshop debris (19,408 items, of which 3,843 are beads); worked antler, including raw material and workshop debris (15,597 items); various forms of burned clay (10,512 items); fragments of casting moulds (7,487 items) and crucibles (3,046 items); iron (7,195 items); and amber (5,087 items). While some finds were made in situ while excavating the layers, the majority were retrieved from wet sieving. All soil from the excavation was sieved using a 4 mm mesh, and almost all layers additionally using a 2 mm mesh.

Analysis of chronologically significant find groups across the A-units and phases shows that some redepositioning has occurred, presumably because of construction work, digging, levelling, and animal burrowing, which could not be fully traced and separated during excavation. In addition, some mixing with material from adjacent units may have occurred during the excavation. Individual finds may therefore have become displaced, and may be registered in both younger and older phases than they originally appeared. A similar risk of redeposition certainly applies to the ecofacts sampled for ^{14}C dating.

Some substantial units, e.g. clay floor layers, may represent construction work undertaken over a few days, while other units may have accumulated over decades of use. Some layers are suspected to comprise material dug up and re-used for levelling. Despite this uncertainty, the general distribution of find types show very consistent, gradual chronological changes through the phases and subphases. This confirms that the majority of the volume of the stratigraphy is associated with a well-defined sequence of deposition.

Selected artefact groups

For the purpose of the present paper, selected artefact groups are traced across the stratigraphy, as their occurrence marks major trends related to the shifting pattern of activities and interactions at the beginning of the Viking Age. While the precise phasing presented here is available only for SJM 3 excavation, general trends are confirmed by earlier excavations in Ribe, including the major excavation ASR 9 Posthuset [64,65].

Glass bead making
Throughout phases F3–F9, Ribe is characterized by a large number of finds of glass debris relating to the manufacture of wound glass beads made from glass cullet (Extended Data Figure 1). These finds mark one of the most active craft industries at the early site. It also marks Ribe's earliest long-distance trade relations, as the glass material was probably imported from derelict Roman sites in the Rhine area or elsewhere in Western Europe. In phases F5-F7, 'Ribe-type' beads are common (Extended Data Figure 1g). In phases F8 and F9, the most distinctive type is so-called 'wasp beads' made of a cylindrical core of mostly dark glass decorated by stripes of applied – usually yellow – glass (hence the similarity to a bee or wasp - Extended Data Figure 1h). This type occurs regularly through all subphases of phases F8 and F9, whereas the number of finds drop steeply in phase F10.

Like the distribution of wasp beads, finds of debris associated with glass-bead working occur throughout phases F8 and F9, but decline steeply in phase F10. The common types of raw materials – tesserae from Roman glass mosaics, splints of coloured glass (possibly also re-melted tesserae), and fragments of broken glass vessels – all occur in the hundreds in phases F8 and F9, while the numbers drop to a few dozen in phase F10, and in subsequent phases to merely occasional, probably largely as re-deposited finds. Similar trends apply to the general glass-working debris, including glass rods used to decorate beads, and ends of rods with plier marks (Table 1).

Non-ferrous metalworking
Debris associated with non-ferrous metalworking occurs in all phases at the site. Until phase F8, however, the types of finds chiefly associated with this activity – crucibles and clay casting moulds – are seen only in very small numbers (Extended Data Figure 2). From phase F9, the number of finds increases dramatically. Somewhat more prolific evidence of earlier non-ferrous metal working is seen in other excavations in Ribe, though never with the same intensity in strata comparable to phases F9–F14.

Apart from marking what was clearly an important new manufacturing activity in the emporium, the significance of the casting moulds is related to the fact that 624 of them bear visible impressions of the objects they were used to cast. In many cases these are distinctive metal ornament types, which are found in graves across Scandinavia and which are key types in the artefact chronologies used to assign a relative dating to these assemblages.

The most common type of metal ornament recognized among the Ribe casting moulds are Berdal-type oval brooches (albeit its strong predominance among the mould fragments is also enhanced by the fact that these were larger than most other objects produced, and thus likely to break into more fragments). The Berdal-type oval brooch is commonly used as a benchmark for the first phase of the Viking Age [66-68]. The date assigned to these and other ornament types is thus directly significant for archaeological assemblages associated with the emergence of the Viking Age across Scandinavia (Table 2). Note that the number of moulds with impressions of Berdal-type brooches are a minimum count, as future analysis may result in further identifications.

From phase F9, 38 mould fragments and 202 crucible fragments can be assigned to one of the six subphases. The great majority of these are associated with the youngest subphase F9e. All 15 fragments of casting moulds for Berdal-type oval brooches from phase F9 were found in two units: A343 and A364. While these cannot be assigned to an exact subphase, they can be confidently associated with the younger subphases d–e (Table 3). These results suggest that the intensification of non-ferrous metalworking and the appearance of Berdal-type oval brooches happened late in phase F9, most likely in the last subphase F9e.

Imported glass beads
With 3,843 finds, glass beads are among the most common artefact finds in the excavation. The majority of beads can be assigned to a limited range of standard types, which also occur widely in Viking-age settlements and graves elsewhere, making them important chronological vectors to relate developments in Ribe to those in archaeology more broadly. During phases F3–F9, when glass-bead making was an important industry at the site, most beads are local products corresponding to the production debris found in the same phases. A chronological succession of preferred bead types can be established over the course of the eighth century [65]. From phase F9 onwards, however, the locally produced

Table 1. Find types associated with glass-bead making from the SJM3 excavation in Ribe. Distribution per main phases. Finds which cannot be assigned to a context are listed as 'unphased', while finds from contexts which may relate to several phases are listed as 'multiple phases'.

Phase	Vessels	Beads	Tesserae	Splints	Debris	Cane ends	Canes	Ribe-type beads	Wasp-type beads
F18	41	34	24	37	23	3	20		1
F17	9	4			2	1	4		
F16	20	21	4		3		3		
F15	12	46	7	3	8	3	2	1	
F14	4	15	4	2			1		
F13	14	50	1	3	3		6		
F12	54	100	2		10	1	3		
F11	40	65	2	5	14	1	5		1
F10	70	190	32	29	64	7	66	1	9
F9	642	965	564	487	147	24	186	3	237
F8	411	128	231	286	77	20	34	6	32
F7	354	300	561	1135	618	245	958	90	5
F6	95	218	435	405	83	15	79	57	
F5/F6	61	329	462	291	275	95	160	33	
F5	134	1081	1088	666	1632	432	405	22	2
F4/F5	29	116	67	71	114	39	49	1	
F4	18	77	24	23	36	10	4	1	
F3	3	10	6	4	9	2			
F2			1		1				
F1				1					
Unphased	**12**	**13**	**5**	**9**	**7**	**1**	**3**		**2**
Mult. phases	**54**	**81**	**90**	**79**	**47**	**5**	**9**	**8**	**4**
Sum	**2077**	**3843**	**3610**	**3536**	**3173**	**904**	**1997**	**223**	**293**

beads are supplemented, and eventually almost replaced, by bead types made elsewhere and acquired through long-distance importation. Most types were probably sourced from the eastern Mediterranean and/or the Middle East [69,70].

The most common type found in Ribe (Extended Data Figure 3) is made from glass tubes, which were drawn and rolled into 'segmented beads'. These can be either plain, coloured glass (of which blue is most commonly found in Ribe), or coated with thin metal foil and various coverings of coloured glass to produce golden, silver, or blue beads [71,72]. The segmented beads were presumably made from rods of some length which were then chopped into individual beads of (typically) one to four segments. This was a highly efficient method of production by which workshops could turn out a large volume of beads compared to the individually made types previously produced in Ribe. This may explain why long-distance procurement was competitive. Many of the segmented beads found in Ribe were faulty pieces lacking a hole or otherwise damaged, which probably implies that they were acquired in large batches and sorted at the destination.

Another type of imported beads, seen almost exclusively in phases F9 and F10, are translucent dark green beads with sides cut into facets, probably in emulation of emerald crystals. Mosaic eye beads are polychrome beads are made by the millefiori technique from multiple coloured glass rods [73]. They are rare in Ribe, and are similarly seen mainly in phases F9 and F10. Small cut tubular beads were made from drawn tubes in the same fashion as segmented beads, but simply chopped into shorter lengths. The chopped pieces were then re-heated to soften the edges. A few of these cut beads appear in phases F9–F11, but they become much more common in phases F12–F13. A less common variety of segmented metal-foil beads were produced from glass blown into shape. A small number of these

Table 2: Find types associated with non-ferrous metal making in the SJM3 excavation in Ribe. Distribution per main phases.

Phase	Crucible fragm.	Moulds no impr.	Moulds w. impr.	of which Berdal
F18	108	192	18	1
F17	33	28		
F16	153	65	4	
F15	225	134	13	
F14	457	1688	70	
F13	194	204	12	4
F12	452	1388	167	36
F11	284	999	176	36
F10	327	566	64	18
F9	333	105	36	10
F8	31	1	3	
F7	34	4	1	
F6	10	2	1	
F5/F6	13	1		
F5	17	1		
F4/F5	5	1		
F4	1	1		
F3	10			
F2		1		
F1				
Mult. Phase	**678**	**1491**	**69**	**8**
Unphased	**54**	**72**	**11**	**5**
Sum	**3419**	**6944**	**645**	**118**

Table 3: Find types associated with non-ferrous metal making in phase F9 subphases. Only a limited proportion of finds from F9 can be assigned to specific subphases.

Subphase	Crucibles	Moulds
e	127	35
d	30	
c	16	1
b	19	2
a	10	

occur from phases F9–F13. With very few exceptions, all imported bead types first appear in phase F9. The three earlier examples are likely to be redeposited pieces (Table 4).

The beads from phase F9 that can be assigned to subphases occur almost exclusively in the last phase, F9e, suggesting that the bead import only took off at this point (Table 5). One clear exception is a rare group of unusually small (< 4 mm wide) segmented metal-foil beads that occur in subphases F9b–d. Besides their small size, these beads differ from other metal-foil beads from the excavation in being produced with a clear layer of glass covering gold foil, rather than amber-coloured glass upon silver foil. This method of production was typical of Roman-period beads, but is very rare in an eighth- or ninth-century context [72]. These beads may mark a separate import unrelated to the major trade flow marked by the other types.

The pattern of bead imports arriving in Ribe in phase F9 closely resembles that seen in other excavations in phases that are likely contemporary (e.g. ASR 9 Posthuset phase F10, cf. [65]: 146–50). After the arrival of the imported bead types, local bead production virtually stops from phase F11 onwards, a fact which indicates that the volume of imported beads arriving must have been substantial.

The range of types corresponds to those seen in other trading sites and in grave assemblages in the Baltic Sea area from the late eighth century at the latest [e.g., 74-76]. As evidence of trade that in some form connected Scandinavia with the Middle East, probably via routes through European Russia, they are one of the artefact groups which reflect the growth of maritime long-distance activities associated with the beginning of the Viking Age.

While the beads can be taken as an indication of long-distance trade, it is unlikely that this trade linked Ribe directly with the source area of the beads. What the beads indicate is the arrival in Ribe of artefact groups that were widely distributed in the Baltic Sea area at approximately the same time. They may thus be interpreted as a proxy for maritime connections with the Baltic Sea area, a view which is substantiated by the numerous affinities between artefact assemblages in contemporary Baltic Sea emporia like Groß Strömkendorf (Reric), Truso, Birka, or Staraya Ladoga [60,74-76].

Rhenish pottery and other Rhine area imports

Imported pottery occurs in all phases in the excavation. While the provenance of some import types has not yet been established, the largest volume of identified imported wares are from the Rhine area (Extended Data Figure 4). The most common of these are the so-called Badorf wares, produced in potteries at Badorf near Cologne in western Germany [77]. Badorf wares occur in most phases, but with a rising volume from phase F9 onwards (Table 6). A variant of Badorf ware, the Reliefband amphorae, are large transport vessels produced in the same workshop area. A small volume of sherds from these occur from phase F9 onwards.

A less common – and less precisely sourced – group of imported pottery is Tating ware. Its precise origin is debated, but was probably somewhere in areas around the Rhine or Meuse Rivers [78]. This black-burnished fine ware was mostly used for large pitchers. It mainly occurs in the excavation from phase F11 onwards. A few earlier sherds from phase F9 and F10 have an atypical appearance, and may relate to other burnished wares.

Another common import in Ribe is rotary quern stones made of basalt from the Niedermendig quarries at Mayen, near Koblenz (and 75 km upstream the Rhine from Cologne). Querns from these quarries were widely distributed in Northern Europe in the Early Middle Ages [79,80]. Like the Badorf ware, they occur in virtually all phases in the excavation, albeit in greater volume from phase F9 and later.

The import of pottery and quern stones reflect Ribe's active contacts with Western Europe. So does the import of raw glass and glass vessels, most of which are likely to have arrived from the same areas (cf. above). Their chronological distribution shows that these contacts existed from the earliest phases of activity in Ribe. They are also the most prolific imports during much of the existence of the trading town. As such, they must mark a pattern of coastal connectivity through the Wadden Sea region to the Rhine, which must have conditioned the early growth of the emporium. As the objects included bulky and heavy items, such as quern stones or amphora, traffic must have been by boat or ship. The growing

Table 4. Common types of imported glass beads in the Northern Emporium excavation in Ribe. Distribution per main phases.

Phase	Small segmented metal foil	Segmented golden metal foil	Segmented clear metal foil	Segmented blue	Segmented blue metal foil	Green faceted	Mosaic eye bead	Small cut tubular	Blown metal foil
F18		3				1		5	
F17			1						
F16		1	1		1			4	
F15			2	1			2	16	
F14						1		3	
F13		3	2					25	
F12		3	1	3	1			65	5
F11		14	3	8		4		8	3
F10		25	7	13		18	4	11	
F9	5	31	3	1	1	10	2	7	1
F8	1							1	
F7		1							
F6									
F5/F6									
F5									
F4/F5									
F4									
F3									
F2									
F1									
Mult. Phases		**7**	**1**			**1**		**11**	
Unphased		**2**		**1**				**2**	
Sum	**6**	**90**	**21**	**27**	**3**	**35**	**8**	**158**	**8**

volume of finds from phase F9 onwards suggest that exchange along this axis intensified at the beginning of the Viking Age.

Scandinavian Peninsula imports

Two groups of imported materials can be identified as products arriving from the Scandinavian Peninsula, and almost certainly from Norway (Extended Data Figure 5). Hones or whetstones made from dark or light schist have been shown by petrographic studies to originate from quarries in Eidsborg in Telemarken and Mostadmarka near Trondheim, Norway [28]. The finds from the SJM3 excavation have yet to undergo petrographic studies, but have been identified visually as similar schists. Apart from a few early finds, which may have been redeposited, they appear from phase F7 onwards (Table 7). From phase F9 larger numbers appear, including fragments which appear to be from the working of raw schist planks into whetstones. The chronological distribution of finds in subphases of phase F9 places this proliferation of finds in the last subphase, F9e (Table 8).

Soap stone or steatite was widely used in Viking-age Norway as a material for carving cooking vessels and for objects such as casting moulds [81]. The vessels were also imported into Denmark on a substantial scale. In the excavation, isolated (hence possibly redeposited) pieces occur in phases F8 and F9, but from phase F10 onwards they occur regularly.

While the materials arriving from Western Europe reflect a coastal sailing pattern that had existed centuries before the Viking Age, the arrival of quantities of stone materials from the Scandinavian Peninsula in a trading site on the west coast of Denmark is likely to reflect maritime transport across open sea. The appearance of these goods probably implies the use of sailing ships on the open North Sea between Norway and Denmark. If so, the finds provide an early proxy for the extension of this technology into Scandinavia.

Table 5. Common types of imported glass beads in phase F9 subphases.

Phase 9 sub-phases	Small seg-mented metal foil	Seg-mented golden metal foil	Seg-mented clear metal foil	Seg-mented blue	Seg-mented blue metal foil	Green faceted	Mosaic eye bead	Small cut tubular	Blown metal foil
e	1	16	1			5	2	3	1
c	1	2				1			
c	2	1							
b	1								
a									

Table 6. Common types of imports from the Rhine area in the SJM3 excavation in Ribe. Distribution per main phases.

Phase	Basalt	Badorf	Reliefband	Burnished incl. Tating
F18	9	13	1	7
F17	11	3		5
F16	62	17	1	2
F15	76	10	1	17
F14	25	6		1
F13	18	15		2
F12	47	47	3	62
F11	2	71		26
F10	26	80	7	9
F9	53	19	2	4
F8	8	5		
F7	6	1		
F6	1			
F5/F6	1	7		
F5	3	6		
F4/F5	4	3		
F4	2			
F3	3			
F2				
F1				
Unphased	**3**	**7**		**2**
Mult. Phases	**47**	**14**	**2**	**22**
Sum	**407**	**324**	**17**	**159**

Table 7. Common types of imports from the Scandinavian Peninsula in the SJM3 excavation in Ribe. Distribution per main phases.

Phase	Schist	Soap stone
F18	20	1
F17	2	5
F16	38	19
F15	14	18
F14	13	13
F13	7	3
F12	15	42
F11	11	39
F10	32	14
F9	79	1
F8	5	1
F7	4	0
F6	1	0
F5/F6	0	0
F5	1	0
F4/F5	0	0
F4	0	0
F3	0	0
F2	0	0
F1	0	0
Unphased	**1**	**1**
Mult. phases	**18**	**45**
Sum	**261**	**202**

Table 8. Finds of schist in phase F9 subphases.

Subphase	Schist
e	35
d	3
c	2
b	4
a	2

Coins
Sixty-three coins were found in the excavations. All are small (c. 11–12 mm in diameter) silver coins known as sceattas (Extended Data Figure 6), widely circulated in the North Sea region in the eighth and early ninth century [82]. From phases F4 to F5, finds of a variety of types occur, including the so-called 'Continental runic' and 'Porcupine' types (Table 9). From phases F5 to F11, however, the pre-dominant coin is the Wodan-Monster type (W/M, also known as Series X). In phases F6–F11, this is virtually the only coin type found, suggesting a controlled circulation.

Table 9. Coin types found in the SJM3 excavation in Ribe. Distribution per main phases. W/M = Wodan/Monster; Cont. runic = continental runic. Total ≠W/M = total number of identified coins that are not W/M (= sum of Porcupine and Continental Runic); ident. Total = total number of identified coins; unid. Total = total number of unidentified coins.

Phase	W/M	Porcupine	Cont. Runic	Total ≠ W/M	Ident. Total	Unid. Total	Total
F18						1	1
F17							
F16							
F15							
F14							
F13							
F12	1				1		1
F11	3				3		3
F10/F11	1				1		1
F10	4				4		4
F9/F10	1				1		1
F9	13				13		13
F8	5				5	1	6
F7	3	1		1	4	1	5
F6	3				3		3
F5/F6	2	1		1	3		3
F5	10	7		7	17		17
F4/F5		1	1	2	2		2
F4		2	1	3	3		3
F3							
F2							
F1							
Sum	**46**	**12**	**2**	**14**	**60**	**3**	**63**

Comparison with the neighbouring excavation ASR 9 Posthuset from 1990-91

While the materials from SJM 3 Posthustorvet represent the activities at and around a single plot in the settlement, the general chronological patterns of artefact succession identified at the site is observed over a wider area of the emporium. In 1990-91 excavations were conducted prior to construction work in the area due south-east of the site of SJM 3 Posthustorvet (Figure S1). Five trenches (M1-M5) were investigated, covering parts of seven building plots and a road area (ASR 9 Posthuset [50]). For each trench, the excavations were conducted in so far as possible by following the stratigraphic sequence of deposits, and the stratigraphy for each trench was synchronized according to 10 main phases, labelled A-J. The materials recovered show a succession of artefact types that closely match that seen at SJM 3 Posthustorvet. This can be illustrated for four major bead groups: 'Ribe type' beads (Extended Data Figure 1g), small cut tubular beads, green faceted beads and segmented beads including metal foil beads (Tables 10-13). 'Ribe type' beads concentrate in phase C, corresponding to phase F5-F7 at SJM3. The imported bead types, meanwhile, make their appearance in phase F, corresponding to F9 and F10 at SJM3. Due to the constraints of the rescue excavation, the stratigraphy could be less consistently separated at ASR 9. Hence the chronological patterns are more diffuse in some trenches, yet the main trends remain the same. For this reason, the absolute dates for artefact occurrence provided at SJM 3 can be assumed to be generally valid for Ribe's emporium.

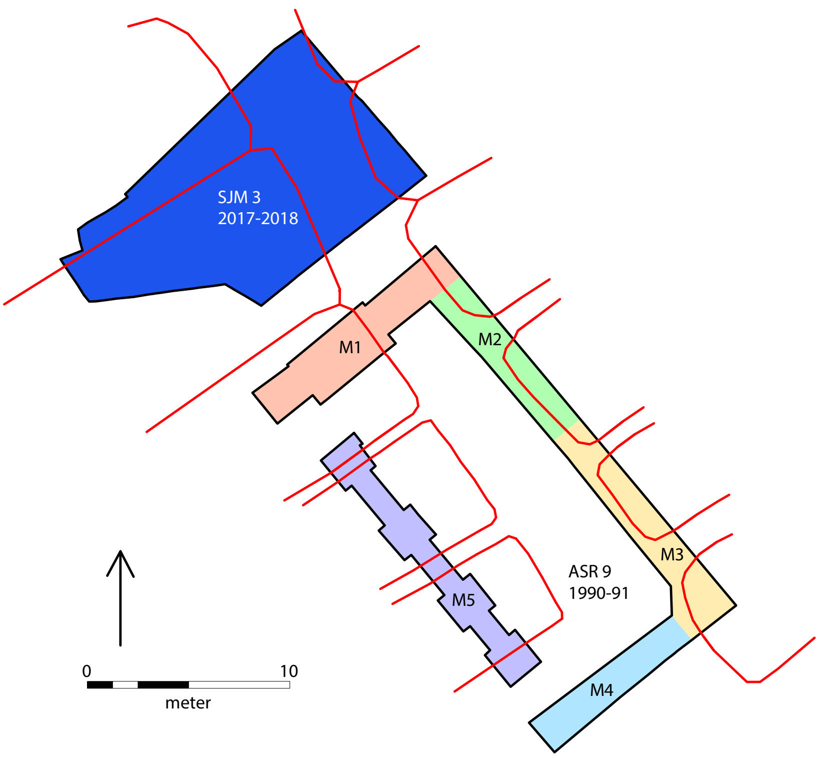

Figure S1. Map of the Northern Emporium excavation (SJM3) of this study and the neighbouring excavation ASR9, excavated in 1990-91, with excavation fields M1 to M5. The plots of the ancient settlement are indicated by red lines.

Table 10. Ribe beads found in the fields M1 to M6 of the excavation ASR9, by stratigraphical phase. Data from [50].

Compare to table 1, find types associated with glass-bead making from the SJM3 excavation in Ribe.

M1+M2		**M3**		**M4**		**M5+M6**		**Total**	
Phase		Phase		Phase		Phase		Phase	
J		J		J		J		J	
No		No		No		No		No	
phase		phase		phase		phase		phase	2
I						I			
		H & I	3	H & I				H & I	7
H	4					H			
G				F, G	1	G		G	
		F & G		& H					
F	1					F		F	1
		E & F							
E				D & E		E	1	E	1
		D & E							
D	6					D	3	D	9
				C & D	1				
C	69	C	46	C	11	C	16	C	142
B	7	B	20	B		B	2	B	29
A		A		A		A		A	
AA		AA		AA		AA		AA	
I alt	87		69		13		22		191
Ribe beads		(extract from Ribe Studier vol 1,2 fig. 9.43)							

Table 11. Segmented beads found in the fields M1 to M6 of the excavation ASR9, by stratigraphical phase. Data from [50].

Compare to table 4, common types of imported glass beads in the Northern Emporium excavation (SJM3).

M1+M2		**M3**		**M4**		**M5**		**Total**	
Phase		Phase		Phase		Phase		Phase	
J		J		J		J		J	
No		No		No		No		No	
phase		phase		phase	2	phase		phase	54
I	1								
		H & I	5	H & I		H & I	18	H & I	26
H	2								
G	26		22	F, G	9	G	22	G	48
		F & G		& H					
F	50					F	5	F	55
		E & F	20						
E	3			D & E	1	E	3	E	6
		D & E							
D						D		D	
				C & D					
C		C		C		C		C	
B	1	B		B		B		B	1
A		A		A		A		A	
AA		AA		AA		AA		AA	
I alt	83		47		12		48		190
Segmented beads		(extract from Ribe Studier vol 1,2 fig. 9.45 and 9.46)							

Table 12. Green faceted beads found in the fields M1 to M6 of the excavation ASR9, by stratigraphical phase. Data from [50].

Compare to table 4, common types of imported glass beads in the Northern Emporium excavation (SJM3).

M1+M2		**M3**		**M4**		**M5**		**Total**	
Phase		Phase		Phase		Phase		Phase	
J	1	J		J		J		J	1
No		No		No		No		No	
phase		phase	7	phase	1	phase		phase	29
I									
		H & I	4	H & I		H & I	10	H & I	16
H	2								
G	10			F, G	5	G	5	G	15
		F & G	8	& H					
F	34					F	2	F	36
		E & F	8						
E	3			D & E		E	1	E	4
		D & E							
D						D		D	
				C & D					
C		C		C	1	C		C	1
B		B		B		B		B	
A		A		A		A		A	
AA		AA		AA		AA		AA	
I alt	50		27		7		18		102
Green faceted			(extract from Ribe Studier vol 1,2 fig. 9.47)						

Table 13. Small cut tubular beads found in the fields M1 to M6 of the excavation ASR9, by stratigraphical phase. Data from [50].

Compare to table 4, common types of imported glass beads in the Northern Emporium excavation (SJM3).

M1+M2		**M3**		**M4**		**M5**		**Total**	
Phase		Phase		Phase		Phase		Phase	
J	1	J		J		J		J	1
No		No		No		No		No	
phase		phase	6	phase		phase		phase	46
I	13								
		H & I	9	H & I		H & I	38	H & I	91
H	31								
G	14			F, G	33	G	1	G	15
		F & G	5	& H					
F	2					F		F	2
		E & F	1						
E	1			D & E		E		E	1
		D & E							
D						D		D	
				C & D	1				
C	1	C		C		C		C	1
B		B		B		B		B	
A		A		A		A		A	
AA		AA		AA		AA		AA	
I alt	63		21		34		39		157
Small cut tubular		(extract from Ribe Studier vol 1,2 fig. 9.49)							

Radiocarbon

Tree-ring record

Oak tree samples (*Quercus* sp.) from three locations in Denmark (Ravning Enge RE, Nybro Søvig Bæk NSB, and Vorbasse VB) were collected and dendrochronologically dated by the tree-ring laboratory at the Danish National Museum. All tree-ring records were dendrochronologically matched with the oak master curves for West Denmark, Sjælland, and Schleswig-Holstein using the program DENDRO for Windows [46] that relies on the methods outlined by Baillie and Pilcher [47]. The investigated pieces of wood originate from four individual trees, with two of them coming from Ravning Enge (RE1 and RE2), and one each from Nybro Søvig Bæk (NSB) and Vorbasse (VB). The samples and radiocarbon results are listed in Table 14.

For examining samples from the period 650–900 CE, the wood was cut into annual samples, further separating early wood (EW) and late wood (LW) wherever possible. Only the late wood samples were pretreated and radiocarbon dated, as early wood can contain carbon from the growing season of the preceding year(s) [48,49]. When the narrowness of the tree rings precluded the separation of early and late wood, we used whole wood (WW) samples.

We extracted α-cellulose from all wood samples [4,50-52]. Samples were bleached at 70°C with 1M sodium chlorite ($NaClO_2$), acidified with 1M hydrochloric acid (HCl), then treated at room temperature with 17% sodium hydroxide (NaOH) to dissolve hemicellulose. Lastly, they were treated with 1M hydrochloric acid at room temperature to remove any atmospheric CO_2 absorbed during the NaOH treatment. Subsequently, the α-cellulose was sealed in glass tubes containing copper oxide (CuO) and combusted to CO_2 at 900°C, cryogenically purified, and converted to graphite using the H_2 reduction method with iron as catalyst [53]. All samples were analysed in the 1MV High Voltage Engineering accelerator mass spectrometer system at the Aarhus AMS Centre, Aarhus University, Denmark [54]. The data presented here is basically bi-annual and each data point based on at least two measurements. The only exceptions are years which yielded insufficient sample material for multiple measurements. In those cases, we also measured one sample from the subsequent year.

Radiocarbon ages are reported as conventional ^{14}C dates in ^{14}C yr BP based on the measured $^{14}C/^{12}C$ ratio corrected for the natural and process isotopic fractionation by normalizing the result to the standard $\delta^{13}C$ value of 25‰ VPDB using the $^{13}C/^{12}C$ ratios measured during AMS analysis [55].

Table 14: Tree ring samples and ^{14}C ages. When no reference is given, the results were obtained in this study. The sample name consists of a site code, the calendar age CE (here denoted "AD"), and WW for whole wood or LW for late wood. NSB = Nybro Søvig Bæk; RE1 and RE2 = Ravning Enge 1 and 2; VB = Vorbasse. Outliers are marked with *.

Lab ID	Name	Year (CE)	^{14}C Age (^{14}C years BP)	dev σ	^{14}C Age$_{mean}$ (^{14}C years BP)	Reference
AAR-24871	NSB 650AD WW	650	1431 ±19 1401 ±16	0.9 -0.8	1413 ±12 (1.5≤3.8)	
AAR-24872	NSB 652AD LW	652	1220 ±19* 1388 ±21	-9.0 0.0	1388 ±21	
AAR-24873	NSB 654AD LW	654	1391 ±18 1370 ±16	0.6 -0.6	1380 ±12 (0.7≤3.8)	
AAR-24874	NSB 656AD LW	656	1411 ±19 1388 ±21	0.5 -0.6	1401 ±14 (0.7≤3.8)	
AAR-24875	NSB 658AD LW	658	1361 ±15 1330 ±29 1341 ±15	0.8 -0.6 -0.5	1348 ±10 (0.6≤3.0)	
AAR-24876	NSB 660AD LW	660	1336 ±16 1340 ±28 1285 ±19	1.1 0.8 -1.8	1319 ±11 (2.5≤3.0)	
AAR-24877	NSB 662AD LW	662	1361 ±16 1367 ±29 1325 ±15	0.9 0.8 -1.3	1345 ±10 (1.6≤3.0)	
AAR-24878	NSB 664AD LW	664	1336 ±15	0.0	1336 ±15	
AAR-24879	NSB 666AD LW	666	1270 ±17	0.0	1270 ±17	
AAR-24880	NSB 668AD LW	668	1270 ±16	0.0	1270 ±16	

Lab ID	Name	Year (CE)	^{14}C Age (^{14}C years BP)	dev σ	^{14}C Age_{mean} (^{14}C years BP)	Reference
AAR-24881	NSB 670AD WW	670	1318 ±19 1338 ±19	-0.5 0.5	1327 ±13 (0.6≤3.8)	
AAR-24882	NSB 672AD LW	672	1286 ±19 1325 ±17 1301 ±15	-1.0 1.2 -0.3	1305 ±9 (1.3≤3.0)	
AAR-24883	NSB 674AD LW	674	1344 ±18 1337 ±15	0.3 -0.2	1340 ±11 (0.1≤3.8)	
AAR-24885	NSB 676AD LW	676	1306 ±18 1310 ±17	-0.2 0.1	1308 ±12 (0.0≤3.8)	
AAR-24887	NSB 678AD LW	678	1305 ±19 1305 ±14	0.0 0.0	1305 ±11 (0.0≤3.8)	
AAR-24889	NSB 680AD LW	680	1281 ±19 1317 ±15	-1.2 0.9	1303 ±11 (2.2≤3.8)	
AAR-24891	NSB 682AD LW	682	1261 ±19 1282 ±15	-0.7 0.6	1273 ±11 (0.7≤3.8)	
AAR-24893	NSB 684AD LW	684	1303 ±18 1275 ±14	0.9 -0.7	1286 ±11 (1.4≤3.8)	
AAR-24895	NSB 686AD LW	686	1306 ±18 1306 ±14	0.0 0.0	1306 ±11 (0.0≤3.8)	
AAR-24897	NSB 688AD LW	688	1305 ±19 1254 ±18	1.4 -1.4	1278 ±13 (3.8≤3.8)	
AAR-24899	NSB 690AD LW	690	1297 ±18 1263 ±16	1.1 -0.9	1278 ±12 (2.0≤3.8)	
AAR-24901	RE1 692AD LW	692	1257 ±19 1267 ±16	-0.3 0.3	1262 ±12 (0.2≤3.8)	[52]
AAR-24903	RE1 693AD LW	693	1284 ±15	0.0	1284 ±15	[52]
AAR-24905	RE1 694AD LW	694	1257 ±16 1289 ±15	-1.0 1.0	1273 ±11 (2.0≤3.8)	[52]
AAR-24907	RE1 695AD LW	695	1320 ±17	0.0	1320 ±17	[52]
AAR-24909	RE1 696AD LW	696	1246 ±15 1221 ±20	0.6 -0.8	1237 ±12 (1.0≤3.8)	[52]
AAR-24911	RE1 697AD LW	697	1306 ±16	0.0	1306 ±16	[52]
AAR-24913	RE1 698AD LW	698	1312 ±14 1185 ±16* 1273 ±12	1.5 -6.7 -1.4	1290 ±9 (4.3≤3.8)	[52]
AAR-24915	RE1 699AD LW	699	1264 ±16	0.0	1264 ±16	[52]
AAR-24917	RE1 700AD LW	700	1304 ±15 1246 ±16* 1302 ±16	0.1 -3.5 -0.1	1303 ±11 (0.0≤3.8)	[52]
AAR-24919	RE1 701AD LW	701	1287 ±15	0.0	1287 ±15	[52]
AAR-24921	RE1 702AD LW	702	1309 ±16 1278 ±16	1.0 -0.9	1293 ±11 (1.9≤3.8)	[52]
AAR-24927	RE1 704AD LW	704	1289 ±16 1306 ±17	-0.5 0.6	1296 ±11 (0.5≤3.8)	[52]
AAR-24929	RE1 706AD LW	706	1276 ±12 1242 ±18	0.9 -1.3	1265 ±10 (2.6≤3.8)	[52]
AAR-24931	RE1 708AD LW	708	1226 ±17 1204 ±16	0.7 -0.6	1214 ±11 (0.9≤3.8)	[52]
AAR-24933	RE1 710AD LW	710	1235 ±15 1220 ±16	0.5 -0.5	1227 ±11 (0.5≤3.8)	[52]
AAR-27088	RE1 712AD WW	712	1273 ±15 1257 ±15	0.5 -0.5	1265 ±10 (0.5≤3.8)	[52]
AAR-27090	RE1 714AD LW	714	1280 ±14 1276 ±17	0.1 -0.1	1278 ±11 (0.0≤3.8)	[52]
AAR-27091	RE1 716AD LW	716	1253 ±13 1226 ±22	0.5 -0.9	1246 ±11 (1.1≤3.8)	[52]
AAR-27092	RE1 718AD LW	718	1261 ±14 1247 ±18	0.4 -0.5	1256 ±11 (0.4≤3.8)	[52]
AAR-27094	RE1 720AD WW	720	1331 ±21* 1248 ±16 1257 ±12	3.7 -0.4 0.2	1254 ±9 (0.2≤3.8)	[52]

Lab ID	Name	Year (CE)	^{14}C Age (^{14}C years BP)	dev σ	^{14}C Age$_{mean}$ (^{14}C years BP)	Reference
AAR-27096	RE1 722AD LW	722	1259 ±23 1242 ±14	0.5 -0.3	1247 ±12 (0.4≤3.8)	[52]
AAR-27098	RE1 724AD LW	724	1264 ±15 1319 ±16* 1240 ±13	0.9 4.3 -0.8	1250 ±10 (1.5≤3.8)	[52]
AAR-27100	RE1 726AD LW	726	1240 ±15 1242 ±17	-0.1 0.1	1241 ±11 (0.0≤3.8)	[52]
AAR-27102	RE1 728AD WW	728	1320 ±14* 1280 ±17 1277 ±13	2.9 0.1 -0.1	1278 ±10 (0.0≤3.8)	[52]
AAR-27104	RE1 730AD WW	730	1308 ±18	0.0	1308 ±18	[52]
AAR-27106	RE1 732AD LW	732	1303 ±15 1279 ±15	0.8 -0.8	1290 ±10 (1.2≤3.8)	[52]
AAR-27108	RE1 734AD LW	734	1287 ±15 1258 ±18	0.7 -0.9	1275 ±11 (1.5≤3.8)	[52]
AAR-27110	RE1 736AD LW	736	1275 ±15 1277 ±15	-0.1 0.1	1276 ±10 (0.0≤3.8)	[52]
AAR-27112	RE1 738AD LW	738	1298 ±20 1279 ±15	0.6 -0.4	1286 ±12 (0.6≤3.8)	[52]
AAR-27113	RE1 740AD LW	740	1302 ±15 1291 ±20	0.2 -0.3	1298 ±12 (0.2≤3.8)	[52]
AAR-27115	RE1 742AD LW	742	1309 ±18 1257 ±16 1258 ±15	2.1 -0.9 -0.9	1272 ±9 (3.0≤3.0)	[52]
AAR-27117	RE1 744AD LW	744	1306 ±16 1304 ±15	0.1 -0.1	1305 ±11 (0.0≤3.8)	[52]
AAR-27119	RE1 746AD LW	746	1300 ±14 1269 ±15	1.0 -1.1	1286 ±10 (2.3≤3.8)	[52]
AAR-27122	RE1 748AD LW	748	1314 ±16 1300 ±15	0.5 -0.4	1306 ±11 (0.4≤3.8)	[52]
AAR-27123	RE1 750AD LW	750	1335 ±15* 1289 ±15 1273 ±14	3.6 0.6 -0.5	1280 ±10 (0.7≤3.8)	[52]
AAR-27125	RE1 752AD LW	752	1308 ±16 1295 ±15	0.4 -0.4	1302 ±11 (0.4≤3.8)	[52]
AAR-27129	RE1 754AD LW	754	1314 ±15 1312 ±16	0.1 -0.1	1313 ±11 (0.0≤3.8)	[52]
AAR-27131	RE1 755AD LW	755	1312 ±15 1327 ±23 1322 ±14 1266 ±14* 1318 ±15 1339 ±16 1319 ±18 1291 ±17 1332 ±20	-0.4 0.4 0.2 -3.7 -0.1 1.2 0.0 -1.6 0.7	1319 ±6 (0.7≤2.0)	[52]
AAR-27132	RE1 756AD LW	756	1318 ±14	0.0	1318 ±14	[52]
AAR-27716	RE1 758AD LW	758	1323 ±19 1306 ±14 1315 ±15	0.5 -0.5 0.1	1313 ±9 (0.3≤3.0)	[52]
AAR-27719	RE1 759AD LW	759	1267 ±20 1377 ±22*	0.0 5.0	1267 ±21	[52]
AAR-27721	RE1 760AD EW	760	1257 ±19	0.0	1257 ±19	[52]
AAR-27723	RE1 760AD LW	760	1288 ±19 1214 ±26	1.3 -1.8	1262 ±15 (5.2≤3.8)	[52]
AAR-27725	RE1 761AD EW	761	1257 ±23	0.0	1257 ±23	[52]
AAR-27727	RE1 761AD LW	761	1321 ±30 1252 ±28	1.2 -1.1	1284 ±21 (2.8≤3.8)	[52]
AAR-27728	RE1 762AD LW	762	1257 ±26 1315 ±18	-1.5 1.1	1296 ±15 (3.3≤3.8)	[52]
AAR-27729	RE1 762AD EW	762	1252 ±19	0.0	1252 ±19	[52]
AAR-27730	RE1 763AD LW	763	1268 ±19 1259 ±46	0.1 -0.2	1267 ±17 (0.0≤3.8)	[52]

Lab ID	Name	Year (CE)	^{14}C Age (^{14}C years BP)	dev σ	^{14}C Age$_{mean}$ (^{14}C years BP)	Reference
AAR-27731	RE1 763AD EW	763	1276 ±24	0.0	1276 ±24	[52]
AAR-27732	RE1 764AD LW	764	1275 ±17 1247 ±27	0.4 -0.8	1268 ±14 (0.8≤3.8)	[52]
AAR-27733	RE1 764AD EW	764	1244 ±19	0.0	1244 ±19	[52]
AAR-27734	RE1 765AD LW	765	1271 ±19 1330 ±21	-1.4 1.6	1297 ±14 (4.5≤3.8)	[52]
AAR-27735	RE1 765AD EW	765	1288 ±19	0.0	1288 ±19	[52]
AAR-27736	RE1 766AD LW	766	1297 ±20 1226 ±26	1.4 -1.7	1270 ±16 (4.8≤3.8)	[52]
AAR-27737	RE1 767AD LW	767	1364 ±24 1345 ±17	0.5 -0.4	1352 ±14 (0.4≤3.8)	[52]
AAR-27739	RE1 768AD LW	768	1249 ±21 1247 ±25	0.0 -0.0	1248 ±16 (0.0≤3.8)	[52]
AAR-27741	RE1 769AD LW	769	1274 ±19 1375 ±31*	0.0 3.3	1274 ±19	[52]
AAR-27743	RE1 770AD LW	770	1282 ±15 1335 ±22	-1.1 1.6	1299 ±12 (4.0≤3.8)	[52]
AAR-27745	RE1 771AD LW	771	1271 ±22 1316 ±24*	0.0 1.9	1271 ±23	[52]
AAR-27748	RE1 772AD LW	772	1273 ±19 1318 ±18	-1.3 1.2	1297 ±13 (2.9≤3.8)	[52]
AAR-27750	RE1 773AD LW	773	1321 ±25 1301 ±33	0.3 -0.4	1313 ±20 (0.2≤3.8)	[52]
AAR-27752	RE1 774AD LW	774	1209 ±22 1210 ±24	0.0 0.0	1209 ±16 (0.0≤3.8)	[52]
AAR-27754	RE1 775AD LW	775	1109 ±23 1118 ±18	-0.2 0.2	1114 ±14 (0.1≤3.8)	[52]
AAR-27755	RE1 776AD LW	776	1135 ±15 1267 ±28*	0.0 4.7	1135 ±15	[52]
AAR-27757	RE1 777AD LW	777	1132 ±26 1096 ±24	0.7 -0.7	1113 ±18 (1.0≤3.8)	[52]
AAR-27758	RE1 778AD LW	778	990 ±19* 1097 ±24	-5.6 0.0	1097 ±24	[52]
AAR-28423	RE1 779AD LW	779	1171 ±32 1146 ±24	0.5 -0.4	1155 ±19 (0.4≤3.8)	[52]
AAR-28425	RE1 780AD LW	780	1209 ±26 1255 ±32*	0.0 1.4	1209 ±26	[52]
AAR-28427	RE1 781AD LW	781	1187 ±22 1110 ±30	1.2 -1.7	1160 ±18 (4.3≤3.8)	[52]
AAR-28428	RE1 782AD LW	782	1165 ±20 1227 ±35*	0.0 1.8	1165 ±20	[52]
AAR-28430	RE1 783AD LW	783	1145 ±19 1135 ±26	0.2 -0.2	1141 ±16 (0.1≤3.8)	[52]
AAR-28432	RE1 784AD LW	784	1148 ±33 1598 ±68*	0.0 6.7	1148 ±32	[52]
AAR-28434	RE1 787AD LW	787	1161 ±19 1209 ±27	-0.8 1.2	1177 ±16 (2.1≤3.8)	[52]
AAR-28436	RE1 788AD LW	788	1184 ±15 1167 ±24	0.3 -0.5	1179 ±13 (0.4≤3.8)	[52]
AAR-28438	RE1 789AD LW	789	1201 ±15 1215 ±32	-0.2 0.3	1204 ±14 (0.2≤3.8)	[52]
AAR-28443	RE1 790AD LW	790	1223 ±19 1206 ±23	0.3 -0.4	1216 ±15 (0.3≤3.8)	[52]
AAR-28445	RE2 792AD LW	792	1192 ±16 1207 ±16	-0.5 0.5	1199 ±11 (0.4≤3.8)	
AAR-28446	RE2 794AD LW	794	1209 ±15 1191 ±16	0.6 -0.6	1200 ±11 (0.7≤3.8)	
AAR-28448	RE2 796AD LW	796	1191 ±19 1194 ±17	-0.1 0.1	1193 ±12 (0.0≤3.8)	

Lab ID	Name	Year (CE)	^{14}C Age (^{14}C years BP)	dev σ	^{14}C Age$_{mean}$ (^{14}C years BP)	Reference
AAR-28449	RE2 798AD LW	798	1207 ±21 1220 ±15	-0.4 0.3	1215 ±12 (0.3≤3.8)	
AAR-28450	RE2 800AD WW	800	1227 ±22	0.0	1227 ±22	
AAR-28452	RE2 802AD LW	802	1199 ±19 1242 ±22	-1.0 1.1	1218 ±14 (2.3≤3.8)	
AAR-28454	RE2 804AD LW	804	1201 ±16 1253 ±17* 1203 ±13	-0.1 3.0 0.1	1202 ±10 (0.0≤3.8)	
AAR-28456	RE2 806AD WW	806	1191 ±17 1739 ±15*	0.0 36.7	1191 ±17	
AAR-28458	RE2 808AD LW	808	1211 ±21 1227 ±16	-0.5 0.4	1221 ±12 (0.4≤3.8)	
AAR-28460	RE2 810AD LW	810	1223 ±16 1245 ±19	-0.6 0.7	1232 ±12 (0.8≤3.8)	
AAR-28462	RE2 812AD LW	812	1206 ±16 1248 ±16	-1.3 1.4	1227 ±11 (3.5≤3.8)	
AAR-28465	RE2 814AD LW	814	1228 ±15 2312 ±15*	0.0 72.3	1228 ±15	
AAR-28466	RE2 816AD LW	816	1240 ±20 1232 ±13	0.3 -0.1	1234 ±11 (0.1≤3.8)	
AAR-28468	RE2 818AD LW	818	1242 ±14 1232 ±14	0.3 -0.3	1237 ±10 (0.2≤3.8)	
AAR-28470	RE2 820AD LW	820	1242 ±14 1234 ±14	0.3 -0.3	1238 ±10 (0.2≤3.8)	
AAR-28472	RE2 822AD LW	822	1173 ±17* 1222 ±15 1203 ±16	-2.4 0.6 -0.6	1213 ±11 (0.7≤3.8)	
AAR-28474	RE2 824AD WW	824	1235 ±15 1212 ±14	0.8 -0.8	1223 ±10 (1.3≤3.8)	
AAR-28476	RE2 826AD LW	826	1227 ±16 1199 ±15	0.9 -0.9	1212 ±11 (1.7≤3.8)	
AAR-28485	RE2 828AD LW	828	1221 ±16 1187 ±19	0.9 -1.1	1207 ±12 (1.9≤3.8)	
AAR-28486	RE2 830AD LW	830	1239 ±14 1213 ±17	0.7 -0.9	1228 ±11 (1.3≤3.8)	
AAR-28505	RE2 832AD WW	832	1250 ±14 1242 ±15	0.3 -0.3	1246 ±10 (0.2≤3.8)	
AAR-28615	VB 832AD LW	832	1198 ±16 1231 ±15	-1.1 1.1	1215 ±11 (2.4≤3.8)	
AAR-28617	RE2 834AD WW	834	1247 ±14 1249 ±15	-0.1 0.1	1248 ±10 (0.0≤3.8)	
AAR-28620	VB 834AD LW	834	1213 ±17	0.0	1213 ±17	
AAR-28622	RE2 836AD WW	836	1232 ±18 1224 ±14	0.3 -0.2	1227 ±11 (0.1≤3.8)	
AAR-28645	VB 836AD LW	836	1200 ±16 1205 ±15	-0.2 0.1	1203 ±11 (0.0≤3.8)	
AAR-28647	RE2 838AD WW	838	1226 ±15 1247 ±17	-0.6 0.7	1235 ±11 (0.9≤3.8)	
AAR-28649	VB 838AD LW	838	1193 ±16 1222 ±17	-0.9 0.9	1207 ±11 (1.6≤3.8)	
AAR-28651	RE2 840AD WW	840	1245 ±20 1240 ±14	0.2 -0.1	1242 ±11 (0.1≤3.8)	
AAR-28653	VB 840AD LW	840	1243 ±18 1236 ±15	0.3 -0.2	1239 ±11 (0.1≤3.8)	
AAR-28655	RE2 842AD WW	842	1216 ±17 1215 ±20	0.0 -0.0	1216 ±13 (0.0≤3.8)	
AAR-28657	RE2 844AD WW	844	1235 ±15* 1187 ±15 1184 ±16	3.3 0.1 -0.1	1185 ±11 (0.0≤3.8)	

Lab ID	Name	Year (CE)	^{14}C Age (^{14}C years BP)	dev σ	^{14}C Age$_{mean}$ (^{14}C years BP)	Reference
AAR-28659	RE2 845AD LW	845	1211 ±17 1212 ±14 1208 ±18 1198 ±19	0.2 0.3 0.0 -0.6	1208 ±8 (0.1≤2.6)	
AAR-28661	RE2 846AD WW	846	1219 ±18 1198 ±19	0.5 -0.6	1210 ±13 (0.6≤3.8)	
AAR-28663	RE2 848AD LW	848	1212 ±15 1204 ±15	0.2 -0.3	1209 ±10 (0.2≤3.8)	
AAR-28665	RE2 852AD WW	852	1224 ±14 1185 ±17	1.1 -1.4	1208 ±11 (3.2≤3.8)	
AAR-28917	RE2 854AD LW	854	1261 ±13* 1179 ±15 1204 ±12	5.1 -1.0 0.8	1194 ±9 (1.7≤3.8)	
AAR-28919	RE2 856AD LW	856	1229 ±19 1206 ±15	0.7 -0.6	1215 ±11 (1.0≤3.8)	
AAR-28921	RE2 858AD LW	858	1246 ±15 1197 ±19 1219 ±13	1.5 -1.5 -0.4	1224 ±8 (2.2≤3.0)	
AAR-28923	RE2 860AD LW	860	1214 ±15 1222 ±16	-0.3 0.2	1218 ±11 (0.1≤3.8)	
AAR-28925	VB 862AD LW	862	1222 ±13	0.0	1222 ±13	
AAR-28927	RE2 862AD LW	862	1233 ±17	0.0	1233 ±17	
AAR-28929	VB 864AD LW	864	1215 ±17 1185 ±17	0.9 -0.9	1200 ±12 (1.6≤3.8)	
AAR-28931	RE2 864AD LW	864	1245 ±15 1218 ±15	0.9 -0.9	1232 ±10 (1.6≤3.8)	
AAR-28933	RE2 866AD LW	866	1221 ±17 1193 ±18	0.8 -0.8	1208 ±12 (1.3≤3.8)	
AAR-28935	RE2 868AD LW	868	1206 ±17 1252 ±14* 1189 ±12	0.7 4.1 -0.5	1195 ±10 (0.7≤3.8)	
AAR-29319	RE2 870AD LW	870	1200 ±14 1221 ±17	-0.6 0.7	1209 ±11 (0.9≤3.8)	
AAR-29325	RE2 872AD LW	872	1165 ±14 1206 ±19	-1.1 1.4	1180 ±11 (3.1≤3.8)	
AAR-29327	RE2 874AD LW	874	1177 ±15 1195 ±17	-0.5 0.6	1185 ±11 (0.6≤3.8)	
AAR-29329	RE2 876AD LW	876	1202 ±16 1234 ±14	-1.1 1.0	1220 ±10 (2.2≤3.8)	
AAR-29331	RE2 878AD LW	878	1148 ±16 1178 ±16	-0.9 0.9	1163 ±11 (1.8≤3.8)	
AAR-29333	RE2 880AD LW	880	1157 ±18 1146 ±19	0.3 -0.3	1152 ±13 (0.2≤3.8)	
AAR-29335	RE2 882AD LW	882	1215 ±21 1102 ±16* 1180 ±14	1.2 -5.7 -0.8	1191 ±11 (2.0≤3.8)	
AAR-29363	RE2 884AD WW	884	1155 ±17 1232 ±15* 1204 ±16	-1.6 3.4 1.5	1181 ±11 (4.6≤3.8)	
AAR-29365	RE2 886AD LW	886	1159 ±14 1185 ±15	-0.9 0.9	1171 ±10 (1.5≤3.8)	
AAR-29959	RE2 888AD LW	888	1154 ±14 1176 ±18	-0.6 0.8	1162 ±11 (1.0≤3.8)	
AAR-29961	RE2 890AD LW	890	1150 ±16 1185 ±18	-0.9 1.1	1165 ±12 (2.1≤3.8)	
AAR-29963	RE2 892AD LW	892	1125 ±15 1167 ±16 1148 ±13	-1.4 1.3 0.1	1146 ±8 (1.9≤3.0)	
AAR-29965	VB 892AD LW	892	1108 ±16 1146 ±13	-1.4 1.2	1130 ±10 (3.5≤3.8)	
AAR-29967	VB 894AD LW	894	1106 ±16 1132 ±16	-0.8 0.8	1119 ±11 (1.4≤3.8)	

Lab ID	Name	Year (CE)	^{14}C Age (^{14}C years BP)	dev σ	^{14}C Age$_{mean}$ (^{14}C years BP)	Reference
AAR-31314	VB 896AD LW	896	1130 ±15 1127 ±16	0.1 -0.1	1129 ±11 (0.0≤3.8)	
AAR-31316	VB 898AD LW	898	1152 ±17 1111 ±18	1.1 -1.2	1133 ±12 (2.7≤3.8)	
AAR-31318	VB 900AD WW	900	1129 ±19 1146 ±13	-0.6 0.4	1141 ±11 (0.6≤3.8)	
AAR-31320	VB 902AD LW	902	1109 ±18 1118 ±13	-0.3 0.3	1114 ±10 (0.2≤3.8)	

Archaeological samples

Samples for radiocarbon dating were selected from excavation phases F3 to F14, as these are the stratified settlement layers (see above for a description of the phases and subphases). The earlier phases F1 and F2 represent the natural subsoil and vegetation surface, while F15 to F18 are heavily bioturbated activity layers from post-Viking Age occupation. The same sequences of layers and artefact types had already been identified in other excavations throughout Ribe [65]. Although it had not been possible to radiocarbon date those sequences, comparisons of the stratigraphies and relative chronologies of this study with earlier excavations ascertains representability of our results for the development of the settlement in general, instead of only being representative for the one plot excavated in this study.

Wherever possible, we radiocarbon-dated at least three samples per context (A-number unit). The risk of redeposited samples was judged to be considerable, in spite of the well-preserved stratigraphy, because of the high intensity of human activities at the urban site. Layers or parts of layers with evidence for massive bioturbation were avoided as well as large homogenous layers that were interpreted as levelling layers, e.g. preparation of a plot after the demolition of a house, which could include substantial amounts of redeposited older material. We targeted short-lived organic material for radiocarbon dating, such as cereal grains, charcoal of young branches, antlers or animal bones. Unfortunately, no articulated animal bones were found in the excavation. Sample selection, dating and modelling was an iterative process that was initiated while the excavation was still on-going. This enabled us to select further samples for the most promising contexts.

Samples suitable for dendrochronological dating were only preserved in phases F4 to F9. In total, we selected 87 samples of oak for dendrochronological and provenance analysis. The analyses were performed by Aoife Daly at Dendro.dk using the program ”DENDRO” [46,83] and for the calculation of the t-value (”t-test”), the program ”CROS” [47]. To estimate the felling dates of the oaks used for the structures on the site, a sapwood average of c. 15–30 sapwood rings was used. Several calculations of the average sapwood in oaks in different regions in Northern Europe have been published, and as the provenance of the oak points towards Denmark, the estimate for Northern Germany (ca. 20 sapwood years (-5+10) [84] was used. In the analysis, master and site chronologies for Northern Europe were consulted.

Some samples of wood were well preserved but did not include enough year rings for dendrochronology. In those cases, we selected two to four samples for radiocarbon wiggle matching. For wiggle matching, several different year rings of a wood or charcoal sample are radiocarbon dated separately. As the year rings between the dated samples are counted, the exact number of years between the different dates of the wiggle match is known. The dates and the numbers of years in between them are combined with OxCal's D_Sequence function.

Samples of charcoal, wood and grains were treated with 1M HCl for one hour at 80°C to remove soil carbonates, 1M NaOH for three hours at 80°C to remove soil humates, and lastly with 1M HCl overnight at room temperature to remove any atmospheric CO_2 absorbed during the NaOH step. Samples were oven-dried at 80°C. Collagen was extracted from bone samples according to the protocol by Longin (1971) with modifications by Brown et al. (1988) and Jørkov et al. (2007) [56-58]. Combustion, graphitisation and measurement were performed as described above.

Table 15: Samples for radiocarbon dating and dendrochronology. See Table 16 for the unmodelled and modelled results of these samples, calibrated with IntCal20 and the Aarhus curve.

Lab ID	Phase (F unit)	Construction (K unit)	Feature (A unit)	Find no. (X no.) and/ or sample no. (P no.)	Material	Species	Comment
AAR-29444	F3	K01	A973	P3161 C	Charcoal	Oak	2 year rings of trunk/branch
AAR-29024	F3	K02	A996	P3157-1	Charcoal	Birch	Wiggle match with AAR-29025 and 29026; outer 2 year rings of a branch with 10-12 year rings, no centre or bark layer preserved
AAR-29025	F3	K02	A996	P3157-2	Charcoal	Birch	Wiggle match with AAR-29024 and 29026; 2 year rings in the middle of a branch with 10-12 year rings, no centre or bark layer preserved
AAR-29026	F3	K02	A996	P3157-3	Charcoal	Birch	Wiggle match with AAR-29024 and 29025; innermost 2 year rings of a branch with 10-12 year rings, no centre or bark layer preserved
AAR-29438	F3	K02	A970	P3121 A	Charcoal	Elder	5-year-old twig
AAR-29439	F3	K02	A970	P3121 B	Charcoal	Birch	5-year-old twig
AAR-29440	F3	K02	A970	P3121 C	Charcoal	Birch	5-year-old twig
AAR-29441	F3	K02	A970	P3121 D	Charcoal	Oak	
Dendro 711-717	F4	K05	A957				
Dendro 716-727	F4	N/A	A932	P03091			
Dendro 723/724	F5	K12	A882				
AAR-29435	F5	K12	A871	X1310, P3000 A	Charcoal	Hazel	1-year-old twig
AAR-29436	F5	K12	A871	X1310, P3000 B	Charcoal	Alder	3 year rings of trunk/branch
AAR-29437	F5	K12	A871	X1310, P3000 C	Charcoal	Alder	3 year rings of trunk/branch
AAR-31325	F6	K15	A690	P2867-I	Wood	Alder	Wiggle match with AAR-31326; year ring no. 1 (the innermost, closest to the centre)
AAR-31326	F6	K15	A690	P2867-II	Wood	Alder	Wiggle match with AAR-31325; year ring no. 22 (the outermost, closest to the bark)
Dendro 720-738	F5	K15 or K16	A644				
AAR-29034	F6	K16	A590	X1227, P2906-1	Grain	Rye	
AAR-29036	F6	K16	A590	X1227, P2906-3	Charcoal	Poplar	
Dendro winter 733/34	F6	K11	A475 and A1111	P3162 and P3191			Two samples with identical age and most probably from the same tree
Dendro 745/746	F7	K17 or K16	A612				Horizontal piece of wood, discarded during the use of K17
Dendro 726-741	F7	K17	A1123				
Dendro 735-746	F7	K17	A1125				
Dendro 729-744	F7	K17 or K36	A497				Could also be assigned to the contemporaneous construction K36.

Lab ID	Phase (F unit)	Construction (K unit)	Feature (A unit)	Find no. (X no.) and/ or sample no. (P no.)	Material	Species	Comment
AAR-29432	F7	K18	A575	P2661 A	Grain	Rye	
AAR-29434	F7	K18	A575	P2661 C	Grain	Barley	
AAR-31398	F7	K19	A443	P2929	Wood	Willow	3 year rings, sampled directly below bark
AAR-31324	F7	K19	A433	P2559	Wood	Hazel	2 year rings, sampled directly below bark
AAR-29429	F8	K20	A403	X1002, P2553 A	Grain	Oat	
AAR-29430	F8	K20	A403	X1002, P2553 B	Charcoal	Elder	3-year-old twig, possibly Elder (Cf. *Sambucus* sp.)
AAR-29431	F8	K20	A403	X1002, P2553 C	Charcoal	Alder	4 year rings of a young branch
AAR-29022	F9	K21	A391	X953, P2507-2	Grain	Rye	
AAR-29023	F9	K21	A391	X953, P2507-3	Grain		
AAR- 28385	F9	K21	A351	P 2477B nr. 2	Charcoal		Wiggle match with AAR-28384, 28595, 28386 and 28387, third to last treering before bark
AAR-28384	F9	K21	A351	P 2477B nr. 1	Organic material		Wiggle match with AAR-28385, 28595, 28386 and 28387, wormhole within the last treering
AAR- 28595	F9	K21	A351	P 2477B nr. 4	Charcoal		Wiggle match with AAR-28384, 28385, 28386 and 28387, last treering before bark
AAR-28386	F9	K21	A351	P 2477B nr. 6	Charcoal		Wiggle match with AAR-28384, 28385, 28387 and 28595, treering no. 15 before bark (measured twice)
AAR- 28387	F9	K21	A351	P 2477B nr. 7	Straw		Wiggle match with AAR-28384, 28385, 28386 and 28595. Straw from bark surface
AAR-28388	F9	K21	A351	P 2477B nr. 8	Grain	Grass	Grass seed from surface of the bark of the twig.
AAR-29043	F9	K21	A377	X938, P2498-1	Grain	Hulled barley	
AAR-29045	F9	K21	A377	X938, P2498-3	Grain		
AAR- 28383	F9	K21	A363	P2462 nr. 7	Charcoal		Wiggle match with AAR-28594 and 28382, treering no. 7 from the bark
AAR- 28594	F9	K21	A363	P2462 nr. 4	Charcoal		Wiggle match with AAR-28383 and 28382, treering no. 4 from the bark
AAR-28382a	F9	K21	A363	P2462 nr. 1	Charcoal		Wiggle match with AAR-28594 and 28383, treering no. 1 from the bark
AAR-29015	F9	K21	A362	X892, P2457-1	Grain	Oat	
AAR-29016	F9	K21	A362	X892, P2457-2	Charcoal	Poplar	
AAR-29017	F9	K21	A362	X892, P2457-3	Charcoal	Alder	
AAR-29426	F9	K21	A354	X861, P2438 A	Charcoal	Poplar	
AAR-29427	F9	K21	A354	P2438 B X861	Charcoal	Alder/ birch	2-3 year rings of trunk/branch of alder/birch (*Alnus/Betula*)
AAR-32115	F9	K21	A357	P2445 X875	Nutshell	Hazel	
AAR-29423	F9	K21	A351	P2428 A	Charcoal	Alder	4 year rings of young branch
AAR-29424	F9	K21	A351	P2428 B	Charcoal	Alder	2-year-old twig

Lab ID	Phase (F unit)	Construction (K unit)	Feature (A unit)	Find no. (X no.) and/ or sample no. (P no.)	Material	Species	Comment
AAR-29425	F9	K21	A351	P2428 C	Charcoal	Willow	1-year-old twig, Cf. Salix
AAR-30137	F9	K21	A351	P2477	Charcoal		1-year-old twig with bark. Measured with high precision.
AAR-29420	F9	K21	A350	X833, P2425 A	Grain	Barley	
AAR-32114	F9	K21	A348	P2382B	Grain	Rye	
AAR-29415	F10	K22	A316	P2363 B	Grain	Rye	
AAR-29416	F10	K22	A316	P2363 C	Charcoal	Hazel	11 year rings of trunk/branch
AAR-29018	F10	K22	A320	P2358-1	Charcoal	Alder	
AAR-29019	F10	K22	A320	P2358-1	Charcoal	Hazel	
AAR-29020	F10	K22	A320	P2358-1	Charcoal	Hazel	
AAR-30136	F10	K22	A294	P0231	Nutshell	Hazel	Measured with high precision.
AAR-29411	F10	K22	A288	P2297 A	Charcoal	Alder	3-year-old twig
AAR-29412	F10	K22	A288	P2297 B	Charcoal	Alder	2 year rings of trunk/branch
AAR-29413	F10	K22	A288	P2297 C	Charcoal	Willow/ poplar	5 year rings of trunk/branch
AAR-29053	F10	K22	A263	P2281-2	Charcoal	Alder	
AAR-29054	F10	K22	A263	P2281-3	Charcoal	Poplar	
AAR-27643	F11	K23	A239	X453A	Bone	Cattle	Calve, radius
AAR-29056	F11	K23	A239	P667-1	Grain	Barley	
AAR-29057	F11	K23	A239	P667-2	Grain	Rye	
AAR-29408	F12	K24	A225	X414, P654 A	Grain	Barley	
AAR-29409	F12	K24	A225	X414, P654 B	Grain	Oat	
AAR-27640	F12	K25	A11	X352A, X352A	Bone	Cattle	Metatarsus
AAR-27634	F12	K25	A165	X323A	Bone	Cattle	Femur
AAR-27633	F12	N/A	A159	X227A	Bone	Cattle	Calve, mandibula
AAR-27629	F13	K26	A135	X179A	Bone	Cattle	Humerus
AAR-29010	F13	K26	A127	P246-2	Grain	Rye	
AAR-29011	F13	K26	A127	P246-3	Charcoal	Birch	
AAR-27622	F13/F14	K26	A114	X146B	Antler	Red deer	With evidence of sawing.
AAR-27621	F13/F14	K26	A114	X146A	Antler	Red deer	With evidence of sawing.
AAR-29012	F13/F14	K26	A101	P169-1	Charcoal	Birch	
AAR-29013	F13/F14	K26	A101	P169-2	Charcoal	Hazel	
AAR-29014	F13/F14	K26	A101	P169-3	Charcoal	Alder	

Lab ID	Phase (F unit)	Construction (K unit)	Feature (A unit)	Find no. (X no.) and/ or sample no. (P no.)	Material	Species	Comment
AAR-29403	F14	K27	A96	P198	Charcoal	Oak	Wiggle match with AAR-29404, ring no. 4
AAR-29404	F14	K27	A96	P198	Charcoal	Oak	Wiggle match with AAR-29403, ring no 22
AAR-31323	F14	K27	A96	N/A	Charcoal	Alder	2 year rings, no bark. Reference sample of the whole layer, therefore no X- or P-number
AAR-29006	F14	K27	A94	X130, P570-1	Grain	Rye	
AAR-29007	F14	K27	A94	X130, P570-2	Grain	Rye	
AAR-29008	F14	K27	A94	X130, P570-3	Grain	Rye	
AAR-27618	F14	K27	A98	X108A	Tooth	Cattle	Calve, deciduous tooth (DP4 sup.)
AAR-29047	F14	K27	A98	P201-2	Grain	Rye	
AAR-30135	F14	K27	A98	Block sample P2695	Charcoal	Alder/ hazel	1-2 year old twig with bark. Measured with high precision.
AAR-30134	F14	K27	A93	Block sample P2695	Charred nutshell	Hazel	Measured with high precision.
AAR-29040	(F14)		A86	X91, P196-3	Grain	Rye	
Plot2							
Dendro 729-744	F7	K36	A497		Wood	Oak	
Dendro 745-760	F9	K38	A387		Wood	Oak	
AAR-27642	F12	N/A	A216	X379A	Bone	Cattle	Metacarpal
AAR-27637	F12	K31	A194	X304A	Cremated bone	Cattle (?)	Phalanx
AAR-27635	F12	K31	A178	X276A	Bone	Cattle	Metatarsal
AAR-27636	F12	K31	A178	X276B	Bone	Cattle	Humerus
AAR-29055	F12	K25	A172	P395	Charcoal	Hazel	
AAR-29042	F12	K31	A178	X276, P396-2	Charcoal	Alder	Wiggle match with AAR-29041
AAR-29041	F12	K31	A178	X276, P396-1	Charcoal	Alder	Wiggle match with AAR-29042
AAR-27632	F13	K31	A158	X224B	Bone	Sheep/ goat	Radius
AAR-27631	F13	K31	A158	X224A	Bone	Cattle	Humerus
AAR-27630	F13	K31	A152	X209A	Bone	Cattle	Tibia
AAR-27627	F13	K31	A130	X197A	Bone	Cattle	Metatarsal
AAR-27628	F13	K31	A130	X197B	Antler	Red deer	Burr of shed antler with traces of sawing
AAR-29406	F14	K32	A124	P234B	Charcoal	Alder/ birch	

Lab ID	Phase (F unit)	Construction (K unit)	Feature (A unit)	Find no. (X no.) and/ or sample no. (P no.)	Material	Species	Comment
Outliers							
AAR-29442	F3	K01	A973	P3161A	Charcoal	Birch	One year ring of branch/trunk
AAR-29443	F3	K01	A973	P3161B	Charcoal	Hazel	One year ring of branch/trunk of possible hazel (Cf. *Corylus*)
AAR-29445	F3	K01	A973	P3161D	Charcoal	Birch	One year ring of branch/trunk of possible birch (Cf. *Betula*)
AAR-29035	F6	N/A	A590	X1227, P2906-2	Charcoal	Alder	
AAR-29433	F7			P2661 B			
AAR-29021	F9	K21	A391	X953, P2507-1	Grain	Hulled barley	
AAR-29044	F9	K21	A377	X938, P2498-2	Grain	Hulled barley	
AAR-29428	F9	K21	A354	P2438 C	Charcoal	Alder	2-3 year rings of trunk/branch
AAR-29421	F9	K21	A350	X833, P2425 B	Grain	Barley	
AAR-29422	F9	K21	A350	X833, P2425 C	Grain		
AAR-29027	F10	K22	A288	X665, P2296-1	Grain	Oat	Uncertain context
AAR-29028	F10	K22	A288	X665, P2296-2	Grain	Hulled barley	Uncertain context
AAR-29029	F10	K22	A288	X665, P2296-3	Charcoal		Diffuse-porous deciduous tree. Uncertain context
AAR-29052	F10		A263	P2281-1	Charcoal	Birch	
AAR-29058	F11	K23	A239	P667-3	Grain	Rye	
AAR-29410	F12	K24	A225	X414, P654 C	Grain	Rye	
AAR-29031	F12	K24	A230	P651-1	Grain	Wheat	
AAR-29032	F12	K24	A230	P651-2	Grain	Rye	
AAR-29033	F12	K24	A230	P651-3	Grain	Rye	
AAR-29049	F12	K25	A11	P617-1	Charcoal	Birch	Layer 5
AAR-29050	F12	K25	A11	P617-2	Charcoal	Birch	Layer 5
AAR-29051	F12	K25	A11	P617-3	Charcoal	Malinae	Layer 5
AAR-27638	F12	K25	A196	X310A	Bone	Cattle	Metatarsal
AAR-27639	F12	K24	A198	X326A	Bone	Cattle	Metacarpal
AAR-27625	F13	K26	A127	X160A	Cremated bone		
AAR-29009	F13	K26	A127	P246-1	Grain	Oat	
AAR-27620	F14	K27	A110	X121A	Antler	Red deer	Burr of shed antler with traces of sawing
AAR-27617	F14	K27	A96	X104A	Antler	Red deer	Burr of shed antler with traces of sawing

Lab ID	Phase (F unit)	Construction (K unit)	Feature (A unit)	Find no. (X no.) and/ or sample no. (P no.)	Material	Species	Comment
AAR-27619	F14	K27	A98	X108B	Antler	Red deer	Antler tine with traces of sawing
AAR-29046	F14	K27	A98	P201-1	Grain	Rye	
AAR-29048	F14	K27	A98	P201-2	Grain	Rye	
AAR-29038	(F14)	N/A	A86	X91, P196-1	Grain	Hulled barley	
AAR-29039	(F14)	N/A	A86	X91, P196-2	Grain	Oat	
AAR-27615	(F14)	N/A	A86	X93A	Antler	Red deer	Antler tine with traces of sawing
AAR-27478	F14	K32	A124	X165	Antler		Part of antler burr
AAR-29405	F14	K32	A124	P243 A	Grain	Rye	
AAR-29407	F14	K32	A124	P243 C	Charcoal	Beech	2 year rings of trunk/branch
AAR-28382b	F9	K21	A363	P2462 nr. 1	Charcoal		Attempted wiggle match with AAR-28594, 28382a and 28383, treering no. 1 from the bark

Annual curve construction

In addition to the latest international calibration curve IntCal20 [6], we measured bi-annual tree-ring data for the period 650–902 CE. The bi-annual ^{14}C tree-ring data covering the periods 650–690 CE and 792–902 CE are not included in the IntCal20 calibration curve and are presented here for the first time (Table 14).

Whenever possible, we measured two radiocarbon dates for each cellulose sample. Selected wide rings were used as an internal reference material, pretreated and dated in several batches. The dates of each tree-ring were reduced to a single measurement per year using a weighted mean value prior to curve construction. Outliers were removed in an iterative process: if the χ^2 statistic for weighted mean value failed for any given year, samples deviating more than ±2.2σ from the weighted mean were discarded. For the curve construction available ^{14}C datasets for 775 CE event are included [2,8,13,34,52,85-88]. Prior to curve construction, the reduced dataset was detrended using a linear fit of degree 1 and normalized using Z-scores. We used Bayesian Functional Data Analysis (BFDA) in order to construct a smoothed annual calibration curve (https://github.com/yjingj/BFDA) [34]. Because the dataset does not contain values for each and every year, the Bayesian framework with Approximations by Basis Functions (BABF) nonstationary data method has been chosen with prior gamma distribution parameters w = 10, ws = 10 and number of knots, m = 42. The optimal number of knots has been estimated using the summed squared Z-scores; see Figure S2. Using a Gaussian distribution with mean and standard deviation taken from the reduced dataset, 1000 functional samples were estimated. The MCMC analysis consisted of 10000 iterations with a burn in of 2000. The lower and upper 95% credible intervals are used for estimating the error on the constructed curve. After the BFDA the resulting smoothed curve is transformed back to original values by reversing the normalization and detrending. Matlab 2020 was used for all data and statistical analysis.

The constructed annual curve is mixed with the IntCal20 curve (Figure S3) for periods, 902–820CE and 720–660CE, where no annual ^{14}C data exists in the IntCal20 dataset [1]. A mixing interval of 10 years is used at each endpoint and the mixing is scaled such that the mixed curve consist of 90% IntCal20 at each endpoint to 0% after 10 years, e.g. 720 CE (90% IntCal20) and 710 CE (0% IntCal20) and 670 CE (0% IntCal20) with 90% IntCal20 at 660 CE.

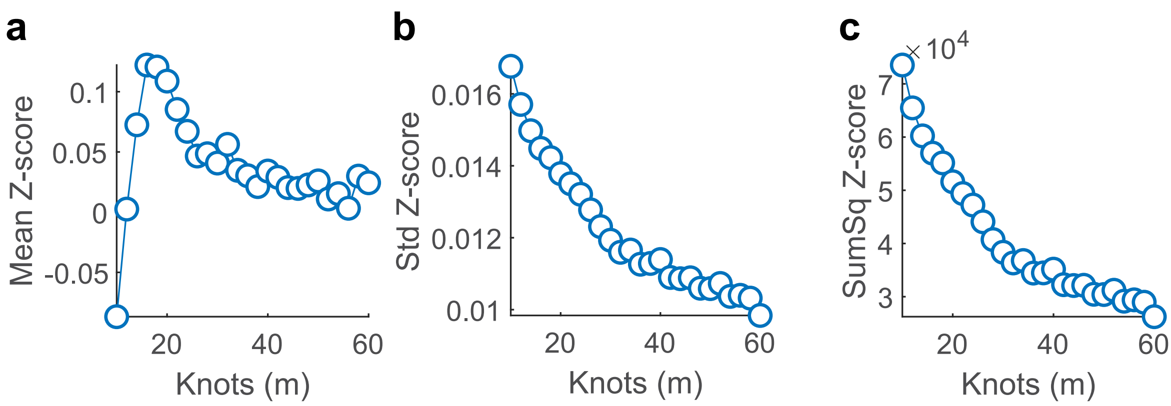

Figure S2. Estimating the number of knots for the Bayesian Functional Data Analysis (BFDA). Z-scores are calculated as the difference from the resulting curve fit and the ^{14}C data divided by the analytical error. a) Mean Z-score. b) Standard deviation of all Z-scores. c) Summed square of Z-scores.

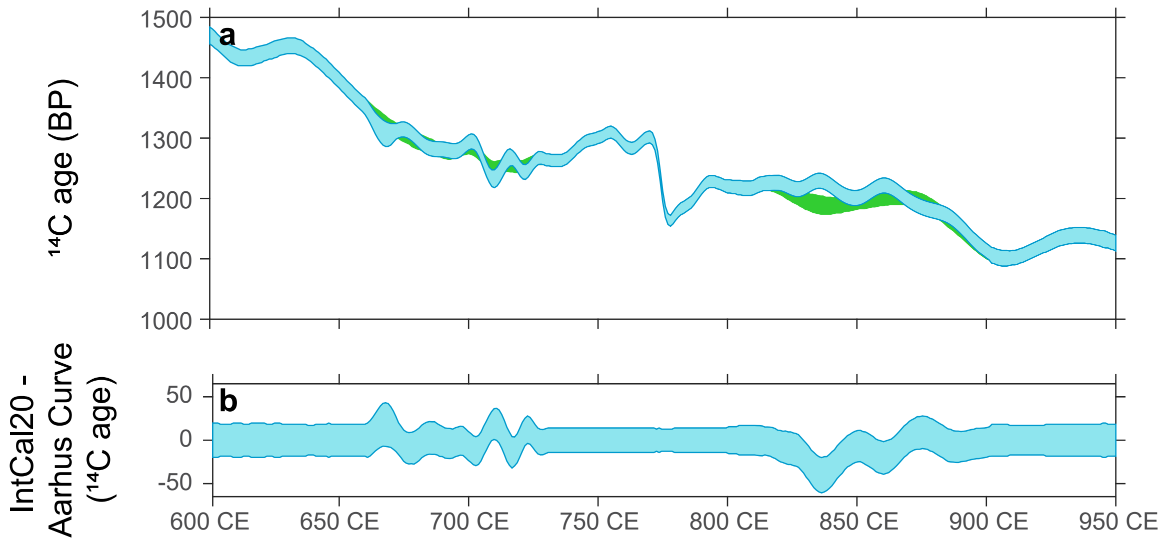

Figure S3. a) Comparison of the Aarhus Curve and IntCal20. b) The difference between the Aarhus Curve and IntCal20, calculated by subtracting the radiocarbon ages of the Aarhus curve from those of IntCal20. While there is a 0 ^{14}C year difference for periods where IntCal20 has annual resolution, the Aarhus curve has more structure, and the difference is about -25 ^{14}C years for the period around 840 CE.

Bayesian modelling of the Ribe chronology

The radiocarbon dates were calibrated in OxCal [37] with an age model according to the excavation stratigraphy. The age model was calculated twice; once with IntCal20 and once with the Aarhus curve (Table 16, Figures 1 and 2 in the main document). We used the Charcoal outlier model (Outlier_Model("Charcoal",Exp(1,-10,0),U(0,3),"t");) with a general prior outlier probability of 0.05. In cases of badly preserved samples or samples from turbated contexts, we used a prior outlier probability of 0.10. In cases of very badly preserved and/or not species-determined samples, as well as heavily turbated contexts, we increased the prior outlier probability to 0.50. Details can be found in the OxCal code provided at the end of the Supplementary Information.

The posterior outlier probabilities are shown in Table 16. Due to the complexity of the stratigraphy and the large number of dates, the models were constructed stepwise. As a first step, simple models were made for 15 out of the 32 identified construction phases (K units), which had yielded radiocarbon samples. The dates were ordered in OxCal's Sequence function according to their position in the stratigraphy. Wiggle matches were calculated when multiple tree rings from wood samples had been dated. Most outliers were already identified in this process. The K units were then arranged in two sequences, one for each of the excavated plots. Boundaries were placed at the transition between archaeological phases (F units). Until phase F12, it was possible to treat the dates from plot 1 and plot 2 in the same sequence. From then on, we had to construct a separate sequence for plot 2. The two sequences for plot 1 and plot 2 could be linked because the phase boundaries F12–F13, F13–F14 and F14–F15 ("End") were identified on both plots. We implemented this using OxCal's Difference function, assuming a difference of 0±20 years between the boundaries from the two different plots.

As an additional illustration of the effect of using different calibration curves, we calibrated selected samples with IntCal13, IntCal20 and the Aarhus curve, without using an age model. As shown in Figure S5, the greatest differences occur between using IntCal13 and any of the annual curves (IntCal20 or Aarhus). For samples on the 9th century plateau, however, there are also differences in the probability distributions of IntCal20 and the Aarhus curve.

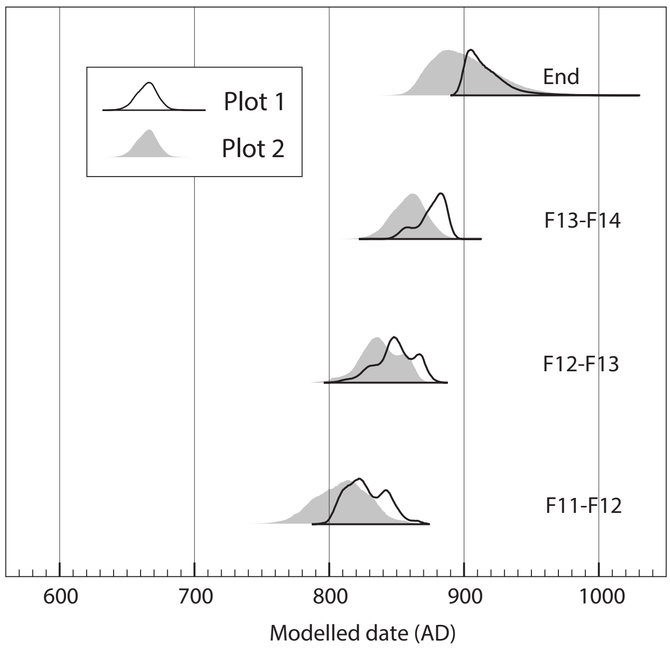

Figure S4. The four boundaries that could be identified on both settlement plots. Boundary End is the boundary between phases F14 and F15, where F14 is the last phase with stratified settlement remains.

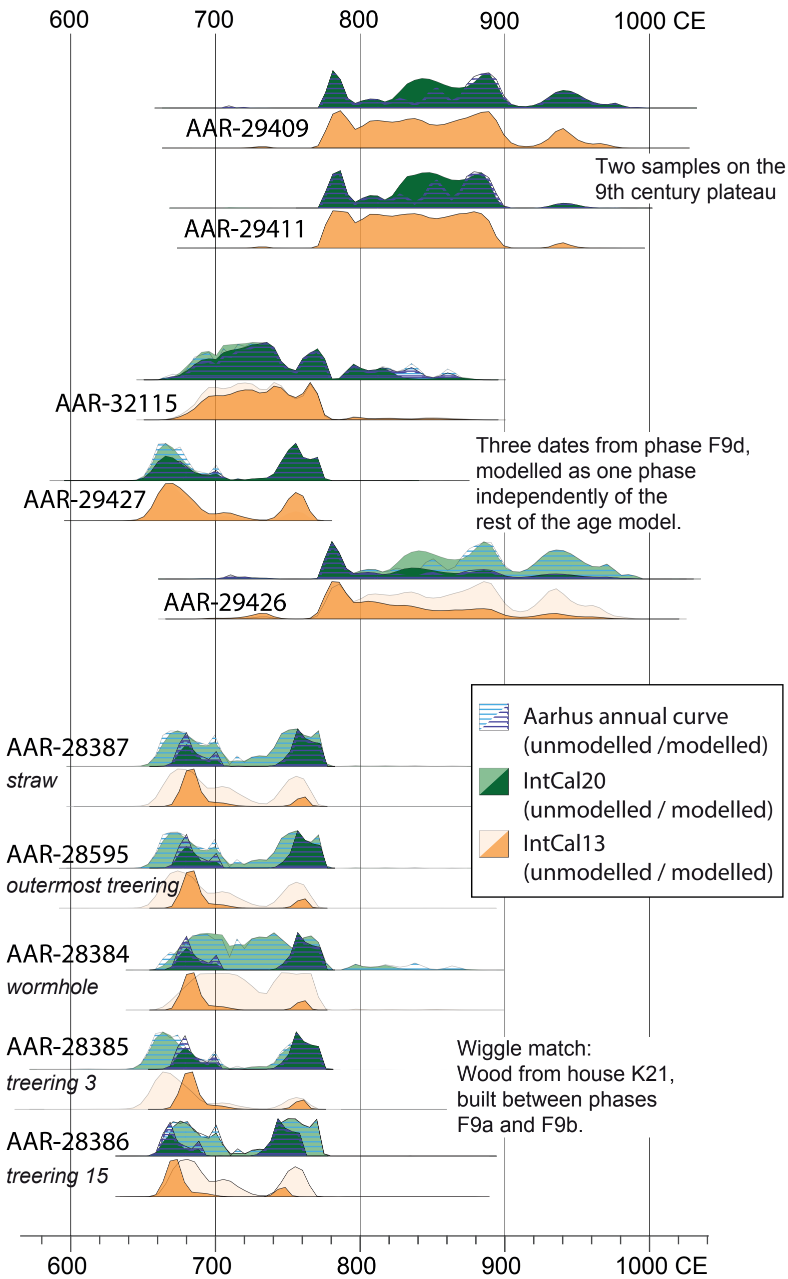

Figure S5. Selected radiocarbon dates of samples from Ribe, calibrated with IntCal13, IntCal20 and the Aarhus curve to exemplify the effect of using different calibration curves.

The wiggle match includes straw that was found embedded in the surface of the wood, the outermost treering, a wormhole within the outermost treering (most likely containing reworked organic material from that treering), and the treerings no. 3 and no. 15.

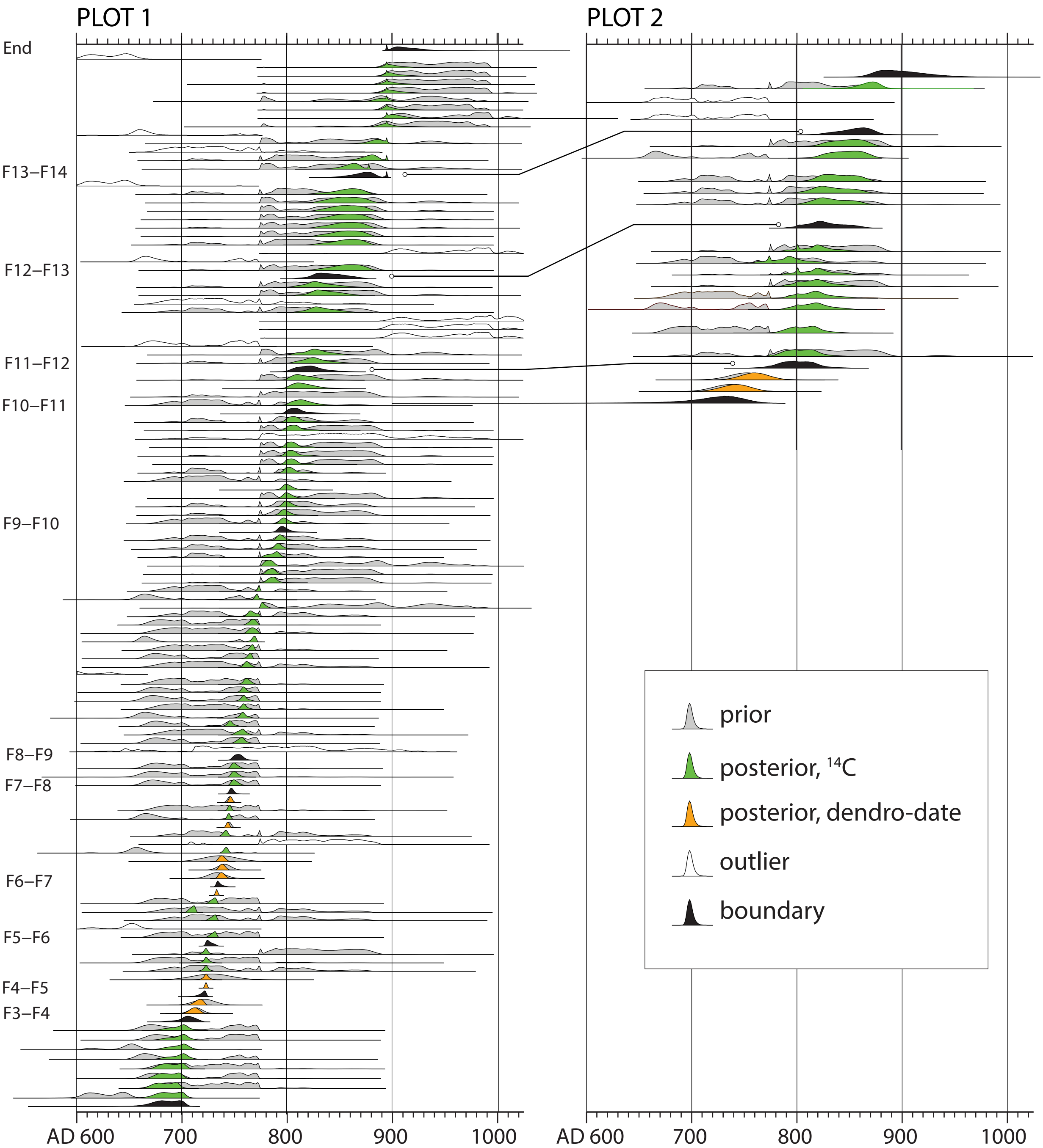

Figure S6. Age model for the excavation SJM 3 in Ribe, calculated with OxCal 4.3.2 [37] and the calibration curve IntCal20 [1] and plotted with MatLab.

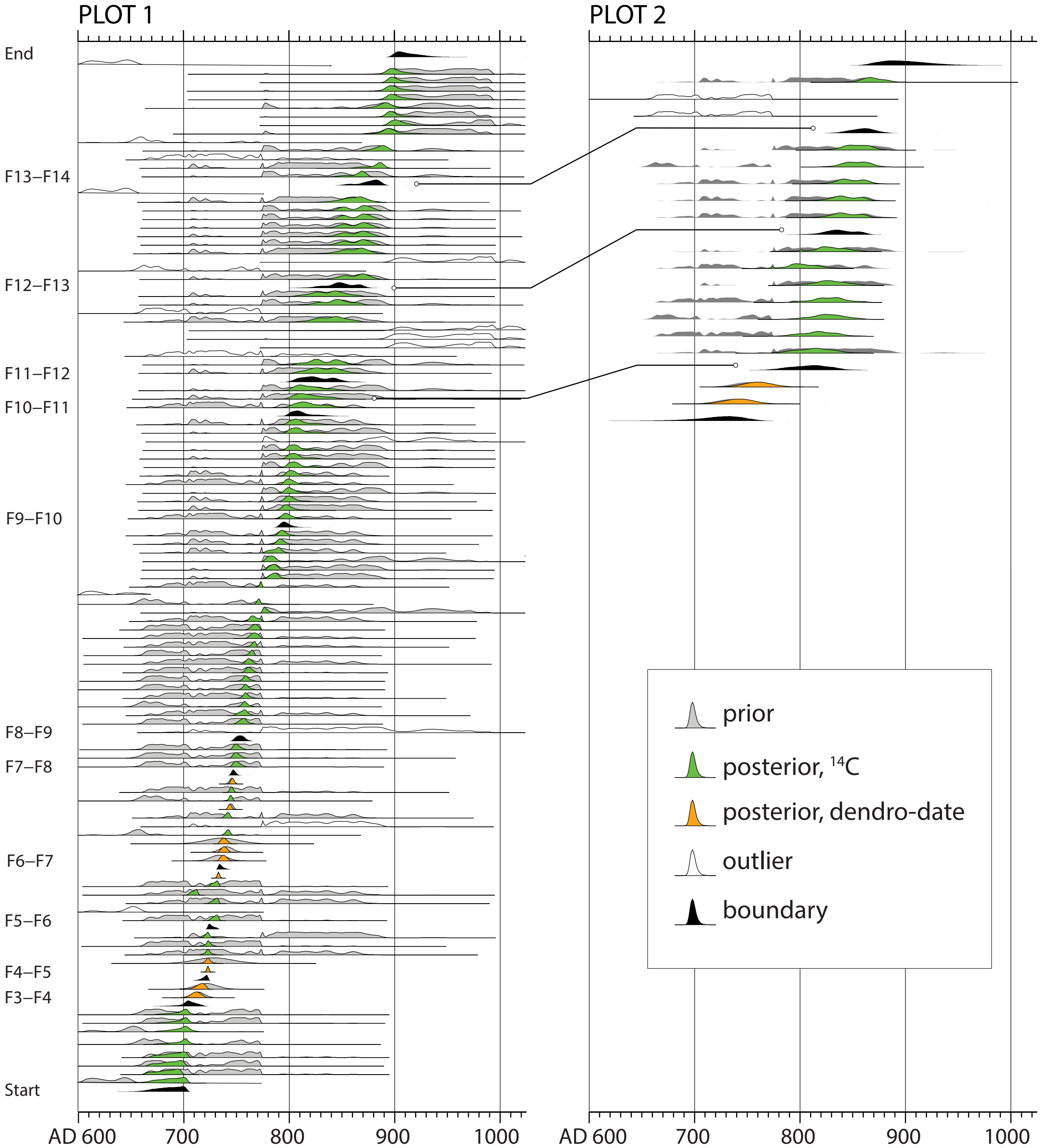

Figure S7. Age model for the excavation SJM 3 in Ribe, calculated with OxCal 4.3.2 [37] and plotted with MatLab. We used the calibration curve "Aarhus curve", where we merged new tree-ring measurements with IntCal20 [1].

Table 16: All radiocarbon dates analysed for this study. Calibrated ages were calculated using OxCal 4.1 with an age model based on the stratigraphy of the site and the Aarhus calibration curve (IntCal20 supplemented with extra bi-annual tree-ring measurements for the period 650-902 CE). In the cases of wiggle matches, we indicate which tree rings were dated. Ten dendrochronology dates are as well included in this table; for these samples, the dating range was converted into one CE date with uncertainty (in the same table column as the ^{14}C ages).

Laboratory ID	^{14}C Age ^{14}C years BP	Calibrated age (68.2% conf.)	Calibrated age (95.4% conf.)	Model agreement	Outlier (posterior/ prior)	Calibrated age (posterior, 68.2% conf.)	Calibrated age (posterior, 95.4% conf.)
Start						677–703 CE [68.3%]	655–706 CE [95.4%]
AAR-29444	1420±23	607–625 CE [37.5%]	601–656 CE [95.4%]	100.8%	99% [*50%*]	682–703 CE [68.2%]	664–705 CE [95.4%]
		637–651 CE [30.7%]					
AAR-29026	1283±24	680 CE – 706 CE [26.2%]	662 CE – 775 CE [94.5%]	105.8%	0% [0%]	677 CE – 689 CE [16.8%]	664 CE – 702 CE [44.3%]
		715 CE – 717 CE [2.1%]	794 CE – 796 CE [0.2%]			695 CE – 700 CE [8.8%]	724 CE – 728 CE [1.4%]
		726 CE – 752 CE [24.1%]	833 CE – 839 CE [0.7%]			739 CE – 749 CE [14.8%]	733 CE – 769 CE [49.7%]
		758 CE – 774 CE [15.8%]				750 CE – 768 CE [27.9%]	665 CE – 700 CE [95.4%]
						678 CE – 698 CE [68.3%]	
AAR-29025	1311±25	663 CE – 684 CE [27.7%]	659 CE – 706 CE [49.0%]	94.3%	0% [0%]	680 CE – 692 CE [16.8%]	667 CE – 705 CE [44.3%]
		699 CE – 704 CE [6.1%]	714 CE – 718 CE [1.4%]			698 CE – 703 CE [8.8%]	727 CE – 731 CE [1.4%]
		743 CE – 762 CE [24.8%]	725 CE – 774 CE [45.1%]			742 CE – 752 CE [14.8%]	736 CE – 772 CE [49.7%]
		765 CE – 773 CE [9.6%]				753 CE – 771 CE [27.9%]	668 CE – 703 CE [95.4%]
						681 CE – 701 CE [68.3%]	
AAR-29024	1282±23	680–706 CE [26.9%]	662–775 CE [94.7%]	110.9%	0% [0%]	683 CE – 695 CE [16.8%]	670 CE – 708 CE [44.3%]
		715–717 CE [2.3%]	834–839 CE [0.7%]			701 CE – 706 CE [8.8%]	730 CE – 734 CE [1.4%]
		726–751 CE [24.1%]				745 CE – 755 CE [14.8%]	739 CE – 775 CE [49.7%]
		758–770 CE [12.0%]				756 CE – 774 CE [27.9%]	671 CE – 706 CE [95.4%]
		771–774 CE [2.9%]				684 CE – 704 CE [68.3%]	
AAR-29438	1334±28	656–681 CE [42.9%]	649–706 CE [61.5%]	91.3%	55% [50%]	696–706 CE [68.2%]	681–710 CE [95.4%]
		701–703 CE [2.0%]	715–717 CE [0.3%]				
		746–760 CE [18.1%]	739–774 CE [33.7%]				
		768–772 CE [5.2%]					
AAR-29439	1385 ±26	613 CE – 615 CE [2.3%]	604 CE – 668 CE [95.4%]	106.2%	NaN% [0%]	690 CE – 708 CE [68.3%]	676 CE – 713 CE [95.4%]
		641 CE – 663 CE [66.0%]					

Laboratory ID	^{14}C Age ^{14}C years BP	Calibrated age (68.2% conf.)	Calibrated age (95.4% conf.)	Model agreement	Outlier (posterior/ prior)	Calibrated age (posterior, 68.2% conf.)	Calibrated age (posterior, 95.4% conf.)
AAR-29440	1303±24	665–686 CE [23.8%]	662–706 CE [46.1%]	99.2%	38% [50%]	697–706 CE [68.2%]	681–708 CE [95.4%]
		698–704 CE [6.8%]	714–718 CE [2.0%]				
		742–773 CE [37.6%]	725–774 CE [47.3%]				
AAR-29441	1317±31	661–686 CE [29.6%]	655–706 CE [50.3%]	98.4%	43% [50%]	691 CE – 707 CE [68.3%]	675 CE – 712 CE [95.4%]
		698–704 CE [6.0%]	714–719 CE [2.0%]				
		743–763 CE [23.4%]	724–774 CE [43.2%]				
		765–773 CE [9.2%]					
Boundary F3-F4						700 CE – 715 CE [68.3%]	685 CE – 721 CE [95.4%]
Dendro F4 K5 A957 711-717	714±6 CE	708–720 CE [68.2%]	702–726 CE [95.4%]	110.7%	0% [0%]	708 CE – 717 CE [68.3%]	704 CE – 721 CE [95.4%]
Dendro F4 A932 716-727	722±10 CE	712–732 CE [68.2%]	702–742 CE [95.4%]	116.1%	0% [0%]	713 CE – 722 CE [68.3%]	709 CE – 724 CE [95.4%]
Boundary F4-F5						718 CE – 724 CE [68.3%]	712 CE – 725 CE [95.4%]
Dendro A882 723/724	724±1 CE	722–725 CE [68.2%]	722–726 CE [95.4%]	101.2%	0% [0%]	723 CE – 725 CE [68.3%]	722 CE – 726 CE [95.4%]
Dendro A644 K12 720-738	729±18 CE	711 CE – 747 CE [68.3%]	693 CE – 765 CE [95.4%]	133.2%	0% [0%]	721 CE – 727 CE [68.3%]	716 CE – 731 CE [95.4%]
AAR-29435	1253±27	684–699 CE [8.9%]	668–670 CE [0.6%]	154.6%	2% [*5%*]	721–727 CE [68.2%]	716–731 CE [95.4%]
		704–743 CE [33.4%]	679–753 CE [49.1%]				
		761–765 CE [2.2%]	758–776 CE [7.8%]				
		773–775 CE [1.8%]	788–870 CE [38.0%]				
		791–802 CE [6.4%]					
		811–822 CE [6.2%]					
		830–841 CE [6.8%]					
		859–864 CE [2.4%]					
AAR-29436	1290±27	667–673 CE [4.5%]	660–775 CE [94.6%]	67.3%	5% [5%]	721 CE – 727 CE [68.3%]	716 CE – 731 CE [95.4%]
		677–705 CE [28.2%]	794–796 CE [0.2%]				
		739–774 CE [35.5%]	834–839 CE [0.6%]				
AAR-29437	1214±27	775–776 CE [0.4%]	706–727 CE [8.4%]	51.7%	2% [*5%*]	720–726 CE [68.2%]	717–731 CE [95.4%]
		787–835 CE [40.7%]	729–738 CE [1.9%]				
		837–870 CE [27.1%]	774–889 CE [85.1%]				
Boundary F5-F6						723–729 CE [68.2%]	723–733 CE [95.4%]

Laboratory ID	^{14}C Age ^{14}C years BP	Calibrated age (68.2% conf.)	Calibrated age (95.4% conf.)	Model agreement	Outlier (posterior/ prior)	Calibrated age (posterior, 68.2% conf.)	Calibrated age (posterior, 95.4% conf.)
AAR-29034	1284 ±22	679 CE – 706 CE [28.7%]	663 CE – 708 CE [39.6%]	94.4%	3% [5%]	728 CE – 734 CE [68.3%]	725 CE – 735 CE [95.4%]
		715 CE – 717 CE [1.9%]	711 CE – 775 CE [55.9%]				
		726 CE – 731 CE [4.1%]					
		737 CE – 753 CE [16.2%]					
		758 CE – 774 CE [17.4%]					
AAR-29036	1247 ±27	694 CE – 697 CE [1.6%]	680 CE – 751 CE [42.5%]	134.5%	3% [5%]	728 CE – 734 CE [68.3%]	725 CE – 735 CE [95.4%]
		705 CE – 741 CE [29.5%]	758 CE – 770 CE [3.5%]				
		773 CE – 775 CE [1.5%]	771 CE – 776 CE [2.4%]				
		790 CE – 824 CE [21.7%]	786 CE – 873 CE [47.0%]				
		828 CE – 842 CE [9.6%]					
		858 CE – 865 CE [4.4%]					
AAR-31325	1255±33	682–700 CE [10.4%]	666–672 CE [1.6%]	137.3%	2% [5%]	681 CE – 685 CE [5.5%]	664 CE – 687 CE [16.2%]
		703–745 CE [31.0%]	677–776 CE [56.7%]			695 CE – 697 CE [1.1%]	692 CE – 700 CE [5.6%]
		760–767 CE [3.4%]	788–870 CE [37.1%]			706 CE – 709 CE [3.5%]	703 CE – 754 CE [73.6%]
		772–775 CE [1.8%]				712 CE – 714 CE [2.2%]	705 CE – 715 CE [95.4%]
		791–803 CE [6.4%]				717 CE – 749 CE [56.0%]	
		811–823 CE [6.2%]				708 CE – 714 CE [68.3%]	
		830–841 CE [6.6%]					
		859–864 CE [2.4%]					
AAR-31326	1296±25	667–674 CE [6.2%]	662–707 CE [43.4%]	63.1%	4% [5%]	701 CE – 705 CE [5.5%]	684 CE – 707 CE [16.2%]
		677–693 CE [17.0%]	713–720 CE [3.8%]			715 CE – 717 CE [1.1%]	712 CE – 720 CE [5.6%]
		697–705 CE [8.4%]	723–774 CE [48.2%]			726 CE – 729 CE [3.5%]	723 CE – 774 CE [73.6%]
		741–773 CE [36.7%]				732 CE – 734 CE [2.2%]	725 CE – 735 CE [95.4%]
						737 CE – 769 CE [56.0%]	
						728 CE – 734 CE [68.3%]	
Dendro A475 and A1111, P3162 and P3191, winter CE 733/34	734 ±1	732 CE – 735 CE [68.3%]	732 CE – 736 CE [95.4%]	100.2%	0% [0%]	733 CE – 735 CE [68.3%]	732 CE – 736 CE [95.4%]
Boundary F6-F7						733 CE – 738 CE [68.3%]	732 CE – 743 CE [95.4%]

Laboratory ID	^{14}C Age ^{14}C years BP	Calibrated age (68.2% conf.)	Calibrated age (95.4% conf.)	Model agreement	Outlier (posterior/ prior)	Calibrated age (posterior, 68.2% conf.)	Calibrated age (posterior, 95.4% conf.)
Dendro A1123 K17 726-741 CE	734±8 CE	726–742 CE [68.2%]	718–750 CE [95.4%]	87.5%	0% [*0%*]	739–746 CE [68.2%]	735–748 CE [95.4%]
Dendro A1125 K17 735-746 CE	741±6 CE	735–747 CE [68.2%]	729–753 CE [95.4%]	122.4%	0% [*0%*]	740–746 CE [68.2%]	736–748 CE [95.4%]
Dendro K36 eller K17 A497 729-744 CE	737±16 cE	721–753 CE [68.2%]	705–769 CE [95.4%]	138.6%	0% [0%]	736 CE – 742 CE [68.3%]	734 CE – 745 CE [95.4%]
AAR-29432	1365 ±26	646 CE – 667 CE [67.2%]	608 CE – 623 CE [3.9%]	84.9%	82% [50%]	741 CE – 745 CE [68.3%]	738 CE – 747 CE [95.4%]
		675 CE – 676 CE [1.0%]	639 CE – 683 CE [82.8%]				
			699 CE – 704 CE [1.0%]				
			745 CE – 760 CE [6.1%]				
			767 CE – 772 CE [1.7%]				
AAR-29434	1244 ±22	705 CE – 740 CE [29.9%]	682 CE – 700 CE [6.4%]	94.7%	60% [50%]	740 CE – 745 CE [68.3%]	738 CE – 746 CE [95.4%]
		773 CE – 775 CE [1.5%]	703 CE – 745 CE [33.1%]				
		791 CE – 806 CE [11.9%]	760 CE – 767 CE [1.6%]				
		810 CE – 824 CE [10.2%]	772 CE – 776 CE [2.1%]				
		829 CE – 842 CE [10.3%]	787 CE – 871 CE [52.2%]				
		858 CE – 865 CE [4.5%]					
Dendro A612 745/746 CE	746±2 CE	743–748 CE [68.2%]	742–750 CE [95.4%]	100.5%	0% [0%]	743 CE – 746 CE [68.3%]	741 CE – 747 CE [95.4%]
AAR-31398	1331±25	657–681 CE [42.4%]	652–705 CE [60.9%]	68.3%	2% [5%]	744 CE – 747 CE [68.3%]	742 CE – 748 CE [95.4%]
		701–703 CE [1.9%]	741–773 CE [34.5%]				
		746–759 CE [18.6%]					
		768–772 CE [5.3%]					
AAR-31324	1278±26	680–706 CE [25.4%]	663–775 CE [89.7%]	115.5%	4% [5%]	744 CE – 748 CE [68.3%]	743 CE – 750 CE [95.4%]
		714–719 CE [4.6%]	792–799 CE [1.4%]				
		724–751 CE [24.9%]	812–822 CE [1.6%]				
		758–770 CE [10.6%]	831–841 CE [2.1%]				
		771–774 CE [2.8%]	860–864 CE [0.6%]				
Boundary F7-F8						746 CE – 750 CE [68.3%]	744 CE – 753 CE [95.4%]
AAR-29429	1312±25	663–684 CE [28.3%]	658–706 CE [50.0%]	130.5%	2% [5%]	747 CE – 754 CE [68.3%]	745 CE – 758 CE [95.4%]
		699–704 CE [5.9%]	714–718 CE [1.3%]				
		743–762 CE [24.5%]	725–732 CE [2.3%]				
		765–773 CE [9.5%]	737–774 CE [41.7%]				
AAR-29430	1311±35	662–691 CE [29.4%]	651–775 CE [95.3%]	132.5%	3% [5%]	747 CE – 754 CE [68.3%]	745 CE – 759 CE [95.4%]
		698–704 CE [6.5%]	835–837 CE [0.1%]				
		742–773 CE [32.3%]					

Laboratory ID	^{14}C Age ^{14}C years BP	Calibrated age (68.2% conf.)	Calibrated age (95.4% conf.)	Model agreement	Outlier (posterior/ prior)	Calibrated age (posterior, 68.2% conf.)	Calibrated age (posterior, 95.4% conf.)
AAR-29431	1303±26	665–690 CE [26.1%]	661–707 CE [45.7%]	129.6%	2% [5%]	747 CE – 754 CE [68.3%]	745 CE – 759 CE [95.4%]
		698–704 CE [6.7%]	713–719 CE [2.6%]				
		742–773 CE [35.4%]	724–774 CE [47.1%]				
Boundary F8-F9						750 CE – 758 CE [68.3%]	747 CE – 763 CE [95.4%]
AAR-29022	1304±23	665–685 CE [24.5%]	662–706 CE [46.6%]	127.8%	5% [10%]	753 CE – 761 CE [68.3%]	749 CE – 766 CE [95.4%]
		698–704 CE [6.7%]	714–718 CE [1.6%]				
		743–763 CE [26.3%]	725–774 CE [47.2%]				
		765–773 CE [10.7%]					
AAR-29023	1260±25	681–701 CE [14.1%]	666–672 CE [1.5%]	56.4%	17% [10%]	753 CE – 761 CE [68.3%]	749 CE – 765 CE [95.4%]
		702–746 CE [39.6%]	678–755 CE [58.5%]				
		760–767 CE [5.0%]	756–775 CE [10.2%]				
		772–775 CE [2.3%]	790–844 CE [21.4%]				
		792–797 CE [2.4%]	855–867 CE [3.8%]				
		816–819 CE [1.4%]					
		832–839 CE [3.5%]					
AAR- 28385	1333±28	656–682 CE [42.0%]	650–706 CE [60.9%]	93.7%	0% [0%]	755 CE – 762 CE [68.3%]	752 CE – 767 CE [95.4%]
(third to last tree-ring before bark)		701–703 CE [2.3%]	715–717 CE [0.3%]				
		746–760 CE [18.4%]	739–774 CE [34.3%]				
		767–772 CE [5.5%]					
AAR-28384	1277±24	681–707 CE [25.9%]	663–775 CE [90.9%]	103.5%	0% [0%]	756 CE – 763 CE [68.3%]	753 CE – 768 CE [95.4%]
(wormhole within the last tree-ring)		713–719 CE [5.0%]	792–798 CE [1.1%]				
		724–750 CE [25.2%]	812–821 CE [1.3%]				
		759–769 CE [9.8%]	831–841 CE [1.8%]				
		771–774 CE [2.4%]	860–862 CE [0.3%]				
AAR- 28595	1312±26	663–684 CE [28.1%]	658–706 CE [49.2%]	112.1%	0% [*0%*]	756 CE – 763 CE [68.3%]	753 CE – 768 CE [95.4%]
(last tree-ring before bark)		699–704 CE [6.0%]	714–718 CE [1.4%]				
		743–762 CE [24.5%]	725–774 CE [44.8%]				
		765–773 CE [9.6%]					
AAR- 28387	1307±25	664–685 CE [25.9%]	661–706 CE [47.5%]	115.5%	0% [*0%*]	756 CE – 763 CE [68.3%]	753 CE – 768 CE [95.4%]
(straw from bark surface)		698–704 CE [6.5%]	714–718 CE [1.6%]				
		743–763 CE [25.6%]	725–774 CE [46.4%]				
		765–773 CE [10.3%]					

Laboratory ID	^{14}C Age ^{14}C years BP	Calibrated age (68.2% conf.)	Calibrated age (95.4% conf.)	Model agreement	Outlier (posterior/ prior)	Calibrated age (posterior, 68.2% conf.)	Calibrated age (posterior, 95.4% conf.)
AAR-29043	1283±22	680–706 CE [26.4%] 715–717 CE [2.1%] 726–752 CE [23.9%] 758–774 CE [15.8%]	663–709 CE [39.3%] 711–775 CE [56.1%]	125.1%	7% [10%]	759 CE – 766 CE [68.3%]	756 CE – 770 CE [95.4%]
AAR-29045	1262±31	680–750 CE [51.0%] 759–769 CE [6.4%] 771–775 CE [2.4%] 792–798 CE [2.8%] 815–819 CE [2.0%] 832–840 CE [3.6%]	665–775 CE [68.6%] 789–845 CE [22.4%] 855–868 CE [4.4%]	105.0%	9% [10%]	759 CE – 766 CE [68.3%]	756 CE – 770 CE [95.4%]
AAR- 28383 (tree-ring no. 7 from the bark)	1305±22	665–685 CE [25.0%] 698–704 CE [6.6%] 743–762 CE [26.2%] 765–773 CE [10.5%]	661–706 CE [47.7%] 714–718 CE [1.5%] 725–732 CE [2.6%] 737–774 CE [43.6%]	104.4%	3% [5%]	763 CE – 768 CE [68.3%]	757 CE – 769 CE [95.4%]
AAR- 28594 (tree-ring no. 4 from the bark)	1270±24	681–708 CE [24.0%] 712–747 CE [34.3%] 759–768 CE [7.6%] 772–774 CE [2.3%]	664–775 CE [85.1%] 791–804 CE [2.9%] 811–823 CE [2.8%] 829–842 CE [3.4%] 858–864 CE [1.2%]	98.9%	5% [5%]	765 CE – 770 CE [68.3%]	759 CE – 771 CE [95.4%]
AAR-28382a	1335 ±15	658 CE – 679 CE [62.2%] 754 CE – 757 CE [6.0%]	653 CE – 684 CE [70.8%] 699 CE – 704 CE [2.8%] 745 CE – 760 CE [17.5%] 767 CE – 772 CE [4.3%]	29.0%	7% [5%]	767 CE – 772 CE [68.3%]	761 CE – 773 CE [95.4%]
AAR-29015	1274±30	679–707 CE [23.1%] 712–752 CE [32.4%] 758–774 CE [12.7%]	663–775 CE [81.8%] 791–824 CE [8.2%] 828–842 CE [3.9%] 858–865 CE [1.6%]	116.4%	9% [*10%*]	764–772 CE [68.2%]	761–774 CE [95.4%]
AAR-29016	1295±22	668–672 CE [4.0%] 678–693 CE [16.7%] 697–705 CE [8.9%] 741–773 CE [38.6%]	663–706 CE [43.6%] 714–719 CE [2.8%] 724–774 CE [49.0%]	124.1%	7% [10%]	765 CE – 772 CE [68.3%]	761 CE – 774 CE [95.4%]

Laboratory ID	^{14}C Age ^{14}C years BP	Calibrated age (68.2% conf.)	Calibrated age (95.4% conf.)	Model agreement	Outlier (posterior/ prior)	Calibrated age (posterior, 68.2% conf.)	Calibrated age (posterior, 95.4% conf.)
AAR-29017	1246±25	705–741 CE [30.4%]	680–749 CE [41.8%]	47.7%	15% [10%]	763 CE – 771 CE [68.3%]	761 CE – 775 CE [95.4%]
		773–775 CE [1.5%]	759–768 CE [2.8%]				
		791–824 CE [22.5%]	772–776 CE [2.3%]				
		829–842 CE [9.6%]	787–872 CE [48.5%]				
		858–865 CE [4.2%]					
AAR-29426	1163±31	775–789 CE [11.6%]	775–792 CE [12.7%]	163.7%	1% [10%]	775 CE – 780 CE [68.3%]	774 CE – 785 CE [95.4%]
		844–855 CE [5.5%]	798–834 CE [8.8%]				
		867–899 CE [26.2%]	838–977 CE [73.9%]				
		921–957 CE [23.9%]					
		970–972 CE [1.0%]					
AAR-29427	1334±26	656–681 CE [44.5%]	651–705 CE [62.4%]	56.5%	34% [10%]	769 CE – 775 CE [68.3%]	767 CE – 783 CE [95.4%]
		701–702 CE [1.3%]	741–773 CE [33.0%]				
		746–759 CE [17.5%]					
		768–772 CE [4.9%]					
AAR-32115	1260±22	682–701 CE [14.2%]	667–672 CE [1.2%]	93.5%	11% [5%]	772 CE – 775 CE [68.3%]	766 CE – 782 CE [95.4%]
		703–745 CE [42.9%]	678–754 CE [62.0%]				
		760–767 CE [4.7%]	757–775 CE [9.8%]				
		772–775 CE [2.3%]	790–843 CE [19.4%]				
		793–796 CE [1.5%]	856–866 CE [3.1%]				
		834–839 CE [2.6%]					
AAR-29423	1204±21	775–776 CE [1.1%]	708–712 CE [2.0%]	113.2%	2% [10%]	782 CE – 791 CE [68.3%]	776 CE – 797 CE [95.4%]
		783–792 CE [8.4%]	774–778 CE [2.2%]				
		798–814 CE [13.6%]	779–888 CE [91.3%]				
		820–832 CE [10.9%]					
		840–875 CE [34.4%]					
AAR-29424	1196±22	775–777 CE [1.9%]	708–712 CE [1.3%]	127.9%	2% [10%]	781 CE – 790 CE [68.3%]	776 CE – 796 CE [95.4%]
		780–791 CE [11.2%]	774–891 CE [94.1%]				
		800–812 CE [8.6%]					
		822–831 CE [7.1%]					
		841–860 CE [18.3%]					
		864–886 CE [21.0%]					

Laboratory ID	^{14}C Age ^{14}C years BP	Calibrated age (68.2% conf.)	Calibrated age (95.4% conf.)	Model agreement	Outlier (posterior/ prior)	Calibrated age (posterior, 68.2% conf.)	Calibrated age (posterior, 95.4% conf.)
AAR-29425	1165±26	775–788 CE [13.8%]	775–792 CE [15.0%]	139.0%	3% [10%]	779 CE – 788 CE [68.3%]	776 CE – 793 CE [95.4%]
		846–854 CE [4.7%]	798–816 CE [3.7%]				
		868–897 CE [29.4%]	818–833 CE [3.4%]				
		924–952 CE [20.4%]	839–904 CE [42.5%]				
			914–976 CE [30.7%]				
AAR-30137	1240±16	706–715 CE [10.1%]	692–697 CE [1.3%]	93.8%	53% [50%]	782 CE – 794 CE [68.3%]	776 CE – 799 CE [95.4%]
		717–726 CE [8.7%]	704–741 CE [30.7%]				
		774–775 CE [1.5%]	773–776 CE [2.0%]				
		791–824 CE [29.4%]	788–870 CE [61.4%]				
		828–842 CE [13.0%]					
		858–865 CE [5.5%]					
AAR-29420	1234±24	706–714 CE [6.5%]	684–699 CE [3.1%]	121.0%	2% [5%]	788 CE – 797 CE [68.3%]	784 CE – 805 CE [95.4%]
		718–724 CE [4.8%]	704–743 CE [23.0%]				
		774–775 CE [1.1%]	762–765 CE [0.4%]				
		789–844 CE [46.9%]	773–776 CE [1.9%]				
		856–867 CE [8.9%]	783–877 CE [66.9%]				
AAR-32114	1242±28	705–739 CE [25.1%]	680–750 CE [36.6%]	122.3%	2% [5%]	790 CE – 799 CE [68.3%]	786 CE – 809 CE [95.4%]
		774–775 CE [1.2%]	759–769 CE [2.6%]				
		790–842 CE [36.7%]	772–776 CE [2.2%]				
		857–865 CE [5.2%]	784–877 CE [54.0%]				
Boundary F9-F10						791 CE – 802 CE [68.3%]	787 CE – 812 CE [95.4%]
AAR-29415	1259±23	682–700 CE [13.4%]	667–672 CE [1.1%]	58.5%	5% [5%]	793 CE – 803 CE [68.3%]	789 CE – 815 CE [95.4%]
		703–745 CE [41.3%]	678–754 CE [59.7%]				
		760–767 CE [4.4%]	757–775 CE [9.5%]				
		772–775 CE [2.3%]	790–844 CE [21.4%]				
		792–797 CE [2.4%]	855–867 CE [3.7%]				
		816–818 CE [1.0%]					
		832–839 CE [3.6%]					
AAR-29416	1217±22	788–846 CE [54.6%]	706–715 CE [4.8%]	122.8%	2% [5%]	793 CE – 804 CE [68.3%]	789 CE – 815 CE [95.4%]
		854–868 CE [13.6%]	717–726 CE [3.0%]				
			733–737 CE [0.7%]				
			774–777 CE [1.8%]				
			780–886 CE [85.1%]				

Laboratory ID	^{14}C Age ^{14}C years BP	Calibrated age (68.2% conf.)	Calibrated age (95.4% conf.)	Model agreement	Outlier (posterior/ prior)	Calibrated age (posterior, 68.2% conf.)	Calibrated age (posterior, 95.4% conf.)
AAR-29018	1228±21	707–712 CE [4.4%]	705–740 CE [17.0%]	127.6%	2% [5%]	795 CE – 807 CE [68.3%]	791 CE – 821 CE [95.4%]
		774–775 CE [0.7%]	773–776 CE [1.8%]				
		789–844 CE [53.2%]	783–878 CE [76.6%]				
		856–867 CE [9.9%]					
AAR-29019	1184±22	775–790 CE [18.3%]	709–710 CE [0.2%]	53.8%	4% [5%]	796 CE – 807 CE [68.3%]	791 CE – 821 CE [95.4%]
		807–810 CE [1.6%]	775–895 CE [91.1%]				
		823–829 CE [3.2%]	929–945 CE [4.1%]				
		842–858 CE [14.9%]					
		864–891 CE [30.2%]					
AAR-29020	1261±24	681–746 CE [56.4%]	666–672 CE [1.6%]	79.1%	55% [50%]	795 CE – 807 CE [68.3%]	791 CE – 821 CE [95.4%]
		759–768 CE [5.4%]	678–775 CE [71.0%]				
		772–775 CE [2.4%]	790–843 CE [19.6%]				
		793–796 CE [1.6%]	856–866 CE [3.2%]				
		834–839 CE [2.5%]					
AAR-30136	1243±15	706–716 CE [12.4%]	687–698 CE [2.9%]	93.3%	35% [50%]	797 CE – 809 CE [68.3%]	793 CE – 826 CE [95.4%]
		717–727 CE [11.9%]	704–742 CE [36.5%]				
		728–738 CE [8.0%]	773–776 CE [2.2%]				
		774–775 CE [1.7%]	789–847 CE [45.2%]				
		791–802 CE [10.1%]	853–869 CE [8.6%]				
		811–822 CE [9.7%]					
		830–841 CE [10.9%]					
		859–864 CE [3.6%]					
AAR-29411	1185±19	775–790 CE [19.6%]	775–894 CE [93.8%]	49.3%	4% [5%]	798 CE – 812 CE [68.3%]	794 CE – 831 CE [95.4%]
		825–828 CE [1.8%]	933–941 CE [1.6%]				
		842–858 CE [15.2%]					
		865–891 CE [31.6%]					
AAR-29412	1199±25	775–777 CE [1.5%]	706–714 CE [2.4%]	104.1%	3% [5%]	798 CE – 812 CE [68.3%]	794 CE – 831 CE [95.4%]
		781–792 CE [9.9%]	719–724 CE [1.1%]				
		799–813 CE [10.8%]	774–893 CE [91.8%]				
		821–832 CE [8.6%]					
		840–883 CE [37.4%]					

Laboratory ID	^{14}C Age ^{14}C years BP	Calibrated age (68.2% conf.)	Calibrated age (95.4% conf.)	Model agreement	Outlier (posterior/ prior)	Calibrated age (posterior, 68.2% conf.)	Calibrated age (posterior, 95.4% conf.)
AAR-29413	1189±20	775–790 CE [18.0%] 807–810 CE [2.0%] 823–829 CE [3.7%] 842–858 CE [16.8%] 864–889 CE [27.9%]	708–711 CE [0.6%] 775–893 CE [94.8%]	66.0%	3% [5%]	798 CE – 812 CE [68.3%]	794 CE – 831 CE [95.4%]
AAR-29053	1191±22	775–791 CE [16.1%] 804–811 CE [5.1%] 823–830 CE [5.0%] 841–859 CE [17.0%] 864–889 CE [25.0%]	708–712 CE [1.1%] 774–894 CE [93.7%] 935–939 CE [0.6%]	79.0%	3% [5%]	798 CE – 817 CE [68.3%]	791 CE – 792 CE [0.5%] 794 CE – 836 CE [95.0%]
AAR-29054	1232±21	707–713 CE [5.6%] 720–723 CE [3.1%] 774–775 CE [0.8%] 790–843 CE [50.2%] 856–866 CE [8.4%]	692–697 CE [1.0%] 704–741 CE [20.8%] 773–776 CE [1.9%] 784–877 CE [71.8%]	120.5%	3% [5%]	798 CE – 817 CE [68.3%]	794 CE – 838 CE [95.4%]
Boundary F10-F11						799 CE – 819 CE [68.3%]	794 CE – 843 CE [95.4%]
AAR-27643	1255±25	683–699 CE [10.4%] 704–744 CE [36.8%] 761–766 CE [2.9%] 773–775 CE [1.9%] 791–799 CE [4.5%] 812–821 CE [4.8%] 831–841 CE [5.6%] 860–863 CE [1.2%]	667–671 CE [0.7%] 679–753 CE [53.2%] 757–776 CE [8.2%] 789–847 CE [27.6%] 853–869 CE [5.7%]	84.1%	48% [50%]	803 CE – 829 CE [68.3%]	798 CE – 848 CE [95.4%]
AAR-29056	1208±30	775–776 CE [0.8%] 785–834 CE [38.8%] 838–874 CE [28.6%]	694–696 CE [0.2%] 705–741 CE [9.9%] 773–894 CE [85.0%] 935–939 CE [0.3%]	118.3%	3% [5%]	803 CE – 830 CE [68.3%]	798 CE – 849 CE [95.4%]
AAR-29057	1186±29	775–791 CE [14.8%] 800–812 CE [7.3%] 821–831 CE [6.1%] 841–860 CE [15.1%] 863–891 CE [24.9%]	707–713 CE [1.6%] 719–723 CE [0.6%] 774–899 CE [85.0%] 922–955 CE [8.1%]	87.4%	3% [5%]	803 CE – 830 CE [68.3%]	799 CE – 849 CE [95.4%]

Laboratory ID	^{14}C Age ^{14}C years BP	Calibrated age (68.2% conf.)	Calibrated age (95.4% conf.)	Model agreement	Outlier (posterior/ prior)	Calibrated age (posterior, 68.2% conf.)	Calibrated age (posterior, 95.4% conf.)
Boundary F11-F12						808 CE – 832 CE [53.2%] 838 CE – 846 CE [15.1%]	801 CE – 855 CE [95.4%]
AAR-29408	1218±22	788–846 CE [54.7%] 854–868 CE [13.5%]	706–715 CE [4.9%] 717–726 CE [3.2%] 733–737 CE [0.7%] 774–777 CE [1.8%] 780–886 CE [84.7%]	114.9%	3% [5%]	819 CE – 849 CE [68.3%]	806 CE – 862 CE [95.4%]
AAR-29409	1172±25	775–790 CE [16.3%] 843–856 CE [9.1%] 866–895 CE [31.2%] 928–947 CE [11.6%]	775–900 CE [76.7%] 919–959 CE [17.7%] 968–973 CE [1.0%]	55.3%	4% [5%]	819 CE – 834 CE [35.8%] 838 CE – 853 CE [32.5%]	805 CE – 860 CE [95.4%]
AAR-27640	1231±32	706–714 CE [5.8%] 718–725 CE [4.8%] 774–776 CE [1.2%] 788–870 CE [56.5%]	681–701 CE [4.8%] 703–745 CE [21.5%] 760–767 CE [1.5%] 772–777 CE [2.2%] 780–887 CE [65.3%]	116.3%	4% [5%]	825 CE – 855 CE [68.3%]	813 CE – 868 CE [95.4%]
AAR-27634	1188±27	775–791 CE [15.4%] 802–812 CE [6.4%] 822–831 CE [5.9%] 841–860 CE [15.8%] 864–890 CE [24.7%]	707–713 CE [1.5%] 720–722 CE [0.4%] 774–896 CE [88.1%] 926–950 CE [5.5%]	104.0%	4% [5%]	828 CE – 835 CE [11.5%] 836 CE – 859 CE [56.7%]	817 CE – 873 CE [95.4%]
AAR-27633	1208±25	775–776 CE [0.7%] 785–793 CE [6.7%] 796–816 CE [17.0%] 817–833 CE [13.3%] 839–873 CE [30.4%]	706–715 CE [3.6%] 718–725 CE [2.1%] 774–891 CE [89.7%]	115.2%	4% [5%]	822 CE – 853 CE [68.3%]	809 CE – 868 CE [95.4%]
Boundary F12-F13						840 CE – 870 CE [68.3%]	820 CE – 876 CE [95.4%]
AAR-27629	1201±24	775–776 CE [1.3%] 782–792 CE [9.5%] 799–813 CE [12.0%] 820–832 CE [9.5%] 840–880 CE [36.0%]	707–713 CE [2.3%] 720–723 CE [0.8%] 774–891 CE [92.2%]	116.2%	4% [5%]	849 CE – 860 CE [24.1%] 862 CE – 878 CE [44.1%]	837 CE – 886 CE [95.4%]

Laboratory ID	^{14}C Age ^{14}C years BP	Calibrated age (68.2% conf.)	Calibrated age (95.4% conf.)	Model agreement	Outlier (posterior/ prior)	Calibrated age (posterior, 68.2% conf.)	Calibrated age (posterior, 95.4% conf.)
AAR-29010	1216±27	775–776 CE [0.5%] 788–849 CE [52.2%] 851–869 CE [15.5%]	705–739 CE [11.7%] 774–778 CE [2.1%] 779–888 CE [81.6%]	104.6%	5% [5%]	851 CE – 876 CE [68.3%]	835 CE – 885 CE [95.4%]
AAR-29011	1194±24	775–777 CE [2.1%] 780–791 CE [11.6%] 800–812 CE [8.2%] 822–831 CE [6.8%] 841–860 CE [17.5%] 864–887 CE [22.0%]	707–713 CE [1.7%] 720–723 CE [0.5%] 774–894 CE [92.7%] 935–939 CE [0.6%]	121.3%	4% [5%]	848 CE – 859 CE [23.9%] 864 CE – 879 CE [44.4%]	839 CE – 886 CE [95.4%]
AAR-27622	1196±28	775–777 CE [1.8%] 780–792 CE [10.3%] 799–813 CE [10.0%] 821–832 CE [8.0%] 840–886 CE [38.1%]	706–714 CE [2.5%] 718–725 CE [1.3%] 774–895 CE [88.8%] 928–947 CE [2.8%]	122.1%	4% [5%]	849 CE – 859 CE [23.7%] 863 CE – 879 CE [44.6%]	838 CE – 886 CE [95.4%]
AAR-27621	1191±24	775–791 CE [15.8%] 802–811 CE [6.1%] 822–830 CE [5.4%] 841–859 CE [16.7%] 864–889 CE [24.2%]	707–712 CE [1.3%] 774–894 CE [92.1%] 931–942 CE [1.9%]	122.4%	3% [5%]	848 CE – 858 CE [23.3%] 864 CE – 880 CE [45.0%]	839 CE – 886 CE [95.4%]
AAR-29012	1184±22	775–790 CE [18.3%] 807–810 CE [1.6%] 823–829 CE [3.2%] 842–858 CE [14.9%] 864–891 CE [30.2%]	709–710 CE [0.2%] 775–895 CE [91.1%] 929–945 CE [4.1%]	119.5%	3% [5%]	847 CE – 857 CE [22.4%] 865 CE – 881 CE [45.9%]	841 CE – 887 CE [95.4%]
AAR-29013	1178±24	775–790 CE [17.7%] 807–810 CE [1.4%] 823–829 CE [2.7%] 842–858 CE [12.7%] 864–894 CE [31.5%] 934–939 CE [2.1%]	709–711 CE [0.3%] 775–898 CE [84.3%] 923–954 CE [10.8%]	117.5%	3% [5%]	847 CE – 857 CE [21.7%] 865 CE – 881 CE [46.6%]	841–887 CE [95.4%]
AAR-29014	1223±22	708 CE – 711 CE [2.5%] 774 CE – 775 CE [0.4%] 789 CE – 845 CE [53.6%] 855 CE – 868 CE [11.8%]	705–738 CE [13.4%] 774–776 CE [1.7%] 782–882 CE [80.4%]	91.8%	6% [5%]	851–875 CE [68.2%]	834–883 CE [95.4%]

Laboratory ID	^{14}C Age ^{14}C years BP	Calibrated age (68.2% conf.)	Calibrated age (95.4% conf.)	Model agreement	Outlier (posterior/ prior)	Calibrated age (posterior, 68.2% conf.)	Calibrated age (posterior, 95.4% conf.)
Boundary F13-F14						870–889 CE [68.2%]	853–892 CE [95.4%]
AAR-29403	1179±26	775–791 CE [16.5%] 804–811 CE [3.5%] 822–830 CE [3.8%] 841–859 CE [13.3%] 864–894 CE [29.3%] 935–939 CE [1.8%]	708–712 CE [0.7%] 775–899 CE [83.4%] 921–956 CE [11.3%]	111.2%	0% [*0%*]	861 CE – 876 CE [68.3%]	845 CE – 878 CE [95.4%]
AAR-29404	1217±21	788–846 CE [54.8%] 854–868 CE [13.4%]	706–715 CE [4.6%] 718–725 CE [2.7%] 774–777 CE [1.8%] 781–886 CE [86.4%]	36.6%	0% [*0%*]	878 CE – 893 CE [68.3%]	862 CE – 895 CE [95.4%]
AAR-31323	1173±25	775–790 CE [16.5%] 843–857 CE [9.8%] 866–895 CE [31.2%] 928–947 CE [10.8%]	775–900 CE [78.1%] 919–958 CE [16.6%] 969–973 CE [0.8%]	126.3%	0% [*0%*]	880 CE – 896 CE [68.3%]	865 CE – 909 CE [92.1%] 918 CE – 934 CE [3.4%]
AAR-27618	1134 ±24	890 CE – 901 CE [11.4%] 918 CE – 962 CE [47.4%] 965 CE – 975 CE [9.5%]	777 CE – 781 CE [2.4%] 880 CE – 991 CE [93.1%]	100.8%	2% [5%]	886 CE – 906 CE [68.3%]	876 CE – 931 CE [95.4%]
AAR-29047	1088 ±22	900–920 CE [25.3%] 957–969 CE [11.3%] 973–994 CE [31.7%]	894–932 CE [34.0%] 942–996 CE [55.4%] 1005–1019 CE [6.0%]	95.9%	1% [5%]	895 CE – 910 CE [68.3%]	890 CE – 924 CE [95.4%]
AAR-30135	1124 ±15	894–902 CE [9.2%] 917–932 CE [18.0%] 941–975 CE [41.1%]	891–979 CE [94.2%] 986–989 CE [1.2%]	97.2%	1% [5%]	890 CE – 907 CE [68.3%]	886 CE – 930 CE [95.4%]
AAR-29006	1151±26	776–784 CE [6.8%] 875–900 CE [22.9%] 920–957 CE [35.9%] 969–973 CE [2.7%]	775–790 CE [9.4%] 843–857 CE [3.2%] 866–991 CE [82.8%]	119.2%	3% [5%]	882 CE – 901 CE [68.3%]	871 CE – 931 CE [95.4%]
AAR-29007	1111±24	896–925 CE [30.5%] 950–980 CE [31.9%] 984–990 CE [5.9%]	892–993 CE [95.4%]	100.6%	1% [5%]	891 CE – 909 CE [68.3%]	884 CE – 929 CE [95.4%]
AAR-29008	1117±24	895–929 CE [33.5%] 945–978 CE [34.7%]	891–992 CE [95.4%]	99.7%	1% [5%]	890 CE – 909 CE [68.3%]	882 CE – 930 CE [95.4%]

Laboratory ID	^{14}C Age ^{14}C years BP	Calibrated age (68.2% conf.)	Calibrated age (95.4% conf.)	Model agreement	Outlier (posterior/ prior)	Calibrated age (posterior, 68.2% conf.)	Calibrated age (posterior, 95.4% conf.)
AAR-30134	1113±17	896–926 CE [33.4%] 950–978 CE [34.8%]	894–991 CE [95.4%]	101.4%	1% [5%]	892 CE – 909 CE [68.3%]	888 CE – 927 CE [95.4%]
AAR-29040	1111±24	896–925 CE [30.5%] 950–980 CE [31.9%] 984–990 CE [5.9%]	892–993 CE [95.4%]	100.6%	1% [5%]	891 CE – 909 CE [68.3%]	884 CE – 929 CE [95.4%]
End of Sequence Plot 1						899 CE – 922 CE [68.3%]	894 CE – 949 CE [95.4%]
Start of Sequence Plot 2						702 CE – 754 CE [68.3%]	625 CE – 627 CE [0.1%] 629 CE – 774 CE [95.3%]
K36 F7 Dendro A497 CE 729-744	737 ±16	721 CE – 753 CE [68.3%]	705 CE – 769 CE [95.4%]	102.8%	0% [0%]	728 CE – 757 CE [68.3%]	713 CE – 770 CE [95.4%]
K38 F9 Dendro A387 CE 745-760	753 ±16	737 CE – 769 CE [68.3%]	721 CE – 785 CE [95.4%]	102.0%	0% [0%]	747 CE – 774 CE [68.3%]	734 CE – 787 CE [95.4%]
Boundary F12-F13 Plot 2						791 CE – 831 CE [68.3%]	770 CE – 846 CE [95.4%]
AAR-27642	1213±35	708 CE – 711 CE [2.0%] 774 CE – 776 CE [1.1%] 784 CE – 875 CE [65.1%]	683–700 CE [2.3%] 703–744 CE [13.7%] 761–766 CE [0.6%] 773–894 CE [77.8%] 931–942 CE [1.0%]	114.7%	36% [50%]	797 CE – 834 CE [68.3%]	775 CE – 777 CE [0.7%] 779 CE – 848 CE [94.7%]
AAR-27637	1279±22	681–706 CE [26.9%] 714–718 CE [3.7%] 725–750 CE [24.9%] 759–769 CE [10.4%] 772–774 CE [2.3%]	663 CE – 775 CE [94.3%] 793 CE – 796 CE [0.3%] 833 CE – 839 CE [0.9%]	81.9%	82% [50%]	804 CE – 838 CE [68.3%]	783 CE – 851 CE [95.4%]
AAR-27635	1319±23	661–683 CE [33.2%] 700–703 CE [4.1%] 745–760 CE [23.1%] 767–772 CE [7.8%]	656–706 CE [54.4%] 715–717 CE [0.4%] 739–774 CE [40.6%]	98.9%	99% [50%]	812 CE – 844 CE [68.3%]	794 CE – 859 CE [95.4%]
AAR-27636	1264±24	681–749 CE [59.2%] 759–768 CE [6.6%] 772–775 CE [2.5%]	666–673 CE [2.0%] 677–775 CE [75.0%] 791–842 CE [16.2%] 858–865 CE [2.1%]	67.7%	58% [50%]	813 CE – 844 CE [68.3%]	795 CE – 860 CE [95.4%]

Laboratory ID	^{14}C Age ^{14}C years BP	Calibrated age (68.2% conf.)	Calibrated age (95.4% conf.)	Model agreement	Outlier (posterior/ prior)	Calibrated age (posterior, 68.2% conf.)	Calibrated age (posterior, 95.4% conf.)
AAR-29055	1209±20	775–776 CE [0.8%] 786–792 CE [6.3%] 797–815 CE [17.3%] 819–832 CE [12.8%] 839–872 CE [31.1%]	707–712 CE [2.6%] 720–722 CE [0.5%] 774–777 CE [1.8%] 780–886 CE [90.5%]	107.0%	37% [50%]	814 CE – 846 CE [68.3%]	797 CE – 860 CE [95.4%]
AAR-29042	1245±26	705 CE – 740 CE [28.0%] 773 CE – 775 CE [1.4%] 790 CE – 842 CE [34.3%] 858 CE – 865 CE [4.6%]	680–750 CE [40.3%] 759–769 CE [2.8%] 772–776 CE [2.3%] 786–873 CE [50.0%]	102.5%	42% [50%]	789 CE – 819 CE [68.3%]	771 CE – 834 CE [95.4%]
AAR-29041	1206±21	775–776 CE [0.9%] 784–792 CE [7.5%] 798–815 CE [15.2%] 819–832 CE [11.8%] 840–874 CE [32.8%]	707–712 CE [2.3%] 721–722 CE [0.3%] 774–777 CE [2.1%] 779–888 CE [90.7%]	105.3%	38% [50%]	816 CE – 846 CE [68.3%]	798 CE – 861 CE [95.4%]
AAR-27632	1235±28	706–715 CE [6.7%] 718–726 CE [5.7%] 732–737 CE [2.4%] 774–775 CE [1.2%] 789–845 CE [43.0%] 855–868 CE [9.2%]	682–700 CE [4.8%] 703–745 CE [23.9%] 760–767 CE [1.3%] 772–777 CE [2.0%] 782–882 CE [63.4%]	112.8%	46% [50%]	830 CE – 850 CE [49.0%] 852 CE – 862 CE [19.2%]	816 CE – 869 CE [95.4%]
AAR-27631	1234±22	706–714 CE [6.6%] 719–724 CE [4.6%] 774–775 CE [1.0%] 790–843 CE [47.6%] 856–866 CE [8.4%]	686–698 CE [2.3%] 704–742 CE [22.9%] 773–776 CE [1.9%] 784–876 CE [68.3%]	109.6%	45% [50%]	830 CE – 849 CE [48.5%] 852 CE – 862 CE [19.7%]	816 CE – 869 CE [95.4%]
AAR-27630	1240±25	706–715 CE [8.0%] 717–726 CE [7.7%] 729–738 CE [6.1%] 774–775 CE [1.1%] 790–842 CE [39.5%] 857–865 CE [5.9%]	682–701 CE [5.7%] 703–745 CE [28.2%] 760–767 CE [1.6%] 772–776 CE [2.1%] 785–875 CE [57.9%]	103.8%	49% [50%]	836 CE – 852 CE [43.2%] 854 CE – 864 CE [25.1%]	823 CE – 872 CE [95.4%]

Laboratory ID	^{14}C Age ^{14}C years BP	Calibrated age (68.2% conf.)	Calibrated age (95.4% conf.)	Model agreement	Outlier (posterior/ prior)	Calibrated age (posterior, 68.2% conf.)	Calibrated age (posterior, 95.4% conf.)
AAR-27627	1332±24	657–681 CE [45.0%] 701–702 CE [0.5%] 747–759 CE [17.8%] 768–772 CE [4.9%]	652–705 CE [61.9%] 742–773 CE [33.5%]	87.8%	100% [50%]	841 CE – 867 CE [68.3%]	828 CE – 878 CE [95.4%]
AAR-27628	1201±23	775–776 CE [1.3%] 782–792 CE [9.6%] 799–813 CE [11.7%] 821–832 CE [9.2%] 840–880 CE [36.4%]	707–712 CE [2.0%] 720–722 CE [0.4%] 774–890 CE [93.0%]	110.4%	42% [50%]	842 CE – 867 CE [68.3%]	828 CE – 878 CE [95.4%]
Boundary F13-F14 Plot 2						847 CE – 872 CE [68.3%]	832 CE – 885 CE [95.4%]
AAR-29406	1227±22	707 CE – 712 CE [4.2%] 774 CE – 775 CE [0.7%] 789 CE – 844 CE [52.8%] 855 CE – 867 CE [10.6%]	705 CE – 740 CE [16.6%] 773 CE – 776 CE [1.8%] 782 CE – 881 CE [77.0%]	69.3%	14% [5%]	858 CE – 881 CE [68.3%]	840 CE – 898 CE [95.4%]
End of Sequence Plot 2						871 CE – 918 CE [68.3%]	859 CE – 953 CE [95.4%]
Outliers							
AAR-29442	2312±25	400 BC – 380 BC [68.3%]	407 BC – 357 BC [88.0%] 275 BC – 259 BC [4.5%] 243 BC – 232 BC [3.0%]	99.9%	0% [*0%*]	400 BC – 380 BC [68.3%]	407 BC – 357 BC [87.9%] 276 BC – 259 BC [4.5%] 243 BC – 232 BC [3.0%]
AAR-29443	2271±24	390 BC – 357 BC [44.7%] 275 BC – 260 BC [13.8%] 242 BC – 232 BC [9.7%]	395 BC – 350 BC [49.6%] 290 BC – 207 BC [45.8%]	99.9%	0% [*0%*]	390 BC – 357 BC [44.3%] 275 BC – 259 BC [14.1%] 242 BC – 232 BC [9.8%]	395 BC – 350 BC [49.7%] 289 BC – 207 BC [45.7%]
AAR-29445	2297±31	399 BC – 360 BC [59.6%] 271 BC – 265 BC [4.3%] 240 BC – 234 BC [4.3%]	406 BC – 351 BC [65.5%] 286 BC – 226 BC [28.2%] 218 BC – 208 BC [1.6%]	100.1%	0% [*0%*]	399 BC – 360 BC [59.5%] 271 BC – 264 BC [4.6%] 240 BC – 234 BC [4.1%]	406 BC – 350 BC [65.5%] 286 BC – 226 BC [28.2%] 218 BC – 208 BC [1.7%]
AAR-29035	1387±23	643–662 CE [68.2%]	606–628 CE [17.4%] 635–666 CE [78.0%]	100.2%	0% [*0%*]	643–661 CE [68.2%]	606–629 CE [17.2%] 635–666 CE [78.2%]
AAR-29433	1204 ±22	775 CE – 776 CE [1.1%] 783 CE – 792 CE [8.4%] 798 CE – 814 CE [13.8%] 819 CE – 832 CE [11.0%] 840 CE – 876 CE [34.0%]	707 CE – 712 CE [2.2%] 721 CE – 722 CE [0.2%] 774 CE – 889 CE [93.0%]	99.8%	0% [0%]	775 CE – 776 CE [1.1%] 783 CE – 792 CE [8.4%] 798 CE – 814 CE [13.8%] 819 CE – 832 CE [11.0%] 840 CE – 876 CE [34.0%]	707 CE – 712 CE [2.2%] 721 CE – 722 CE [0.2%] 774 CE – 889 CE [93.0%]
AAR-29021	1184±43	775–894 CE [66.6%] 935–939 CE [1.6%]	705–739 CE [6.4%] 774–977 CE [89.0%]	99.9%	0% [*0%*]	775–894 CE [66.6%] 934–939 CE [1.6%]	705–739 CE [6.5%] 773–977 CE [88.9%]

Laboratory ID	^{14}C Age ^{14}C years BP	Calibrated age (68.2% conf.)	Calibrated age (95.4% conf.)	Model agreement	Outlier (posterior/ prior)	Calibrated age (posterior, 68.2% conf.)	Calibrated age (posterior, 95.4% conf.)
AAR-29044	833±21	1181–1187 CE [6.8%] 1212–1233 CE [34.8%] 1240–1261 CE [26.6%]	1169 CE – 1171 CE [0.6%] 1175 CE – 1197 CE [15.9%] 1199 CE – 1266 CE [79.0%]	99.9%	0% [*0%*]	1181–1187 CE [6.6%] 1212–1233 CE [35.0%] 1240–1261 CE [26.6%]	1169 CE – 1171 CE [0.6%] 1175 CE – 1197 CE [15.9%] 1199 CE – 1266 CE [79.0%]
AAR-28382	1363 ±25	647 CE – 667 CE [67.6%] 675 CE – 676 CE [0.7%]	609 CE – 620 CE [2.4%] 640 CE – 683 CE [84.0%] 699 CE – 704 CE [1.0%] 745 CE – 760 CE [6.4%] 767 CE – 772 CE [1.7%]	100.2%	0% [0%]	647 CE – 667 CE [68.3%]	609 CE – 620 CE [2.3%] 640 CE – 683 CE [84.2%] 699 CE – 704 CE [1.0%] 745 CE – 760 CE [6.3%] 767 CE – 772 CE [1.6%]
AAR-29428	1508±33	547–601 CE [68.2%]	439–462 CE [3.7%] 478–497 CE [4.4%] 533–643 CE [87.3%]	100.0%	0% [*0%*]	547–600 CE [68.2%]	439–461 CE [3.7%] 478–498 CE [4.3%] 534–643 CE [87.4%]
AAR-29421	595±21	1321–1358 CE [56.9%] 1391–1398 CE [11.3%]	1306–1365 CE [74.2%] 1384–1406 CE [21.2%]	100.0%	0% [*0%*]	1321–1358 CE [57.2%] 1391–1398 CE [11.0%]	1306–1365 CE [74.1%] 1384–1406 CE [21.3%]
AAR-29422	784±23	1229–1246 CE [33.3%] 1255–1272 CE [34.9%]	1223–1276 CE [95.4%]	100.0%	0% [*0%*]	1229–1246 CE [33.2%] 1255–1272 CE [35.0%]	1223–1276 CE [95.4%]
AAR-29414	871 ±23	1168 CE – 1216 CE [68.3%]	1053 CE – 1077 CE [6.0%] 1156 CE – 1224 CE [89.4%]	99.8%	0% [0%]	1168 CE – 1216 CE [68.3%]	1053 CE – 1077 CE [6.0%] 1156 CE – 1224 CE [89.4%]
AAR-29027	745±26	1263–1285 CE [68.2%]	1228–1250 CE [14.5%] 1253–1293 CE [80.9%]	99.6%	0% [*0%*]	1263–1286 CE [68.2%]	1227–1249 CE [14.6%] 1252–1293 CE [80.8%]
AAR-29028	289±31	1523–1575 CE [46.5%] 1629–1652 CE [21.7%]	1497–1602 CE [63.0%] 1612–1662 CE [31.4%] 1788–1793 CE [1.0%]	100.0%	0% [*0%*]	1523–1575 CE [46.5%] 1629–1652 CE [21.7%]	1497–1601 CE [63.2%] 1614–1662 CE [31.2%] 1788–1793 CE [1.0%]
AAR-29029	842±22	1177–1194 CE [21.9%] 1201–1228 CE [40.6%] 1247–1254 CE [5.7%]	1166–1262 CE [95.4%]	100.0%	0% [*0%*]	1177–1194 CE [21.9%] 1201–1228 CE [40.6%] 1247–1254 CE [5.7%]	1166–1235 CE [78.1%] 1238–1261 CE [17.3%]

Laboratory ID	^{14}C Age ^{14}C years BP	Calibrated age (68.2% conf.)	Calibrated age (95.4% conf.)	Model agreement	Outlier (posterior/ prior)	Calibrated age (posterior, 68.2% conf.)	Calibrated age (posterior, 95.4% conf.)
AAR-29052	1158 ±23	776 CE – 786 CE [11.3%] 872 CE – 898 CE [28.5%] 923 CE – 953 CE [28.5%]	775 CE – 790 CE [13.1%] 806 CE – 810 CE [0.4%] 823 CE – 829 CE [0.8%] 842 CE – 859 CE [4.9%] 864 CE – 977 CE [76.3%]	99.8%	0% [0%]	776 CE – 786 CE [11.2%] 872 CE – 898 CE [28.6%] 923 CE – 953 CE [28.5%]	775 CE – 790 CE [13.1%] 806 CE – 810 CE [0.4%] 823 CE – 829 CE [0.8%] 842 CE – 859 CE [4.9%] 864 CE – 977 CE [76.3%]
AAR-29058	527±22	1406–1425 CE [68.2%]	1328–1336 CE [2.5%] 1396–1438 CE [92.9%]	99.9%	0% [*0%*]	1406–1425 CE [68.2%]	1328–1336 CE [2.5%] 1396–1438 CE [92.9%]
AAR-29410	380±24	1457–1503 CE [51.0%] 1599–1617 CE [17.2%]	1449–1524 CE [64.0%] 1574–1630 CE [31.4%]	100.0%	0% [*0%*]	1457–1503 CE [51.1%] 1599–1617 CE [17.1%]	1450–1523 CE [64.0%] 1574–1630 CE [31.4%]
AAR-29031	1090±23	899–921 CE [25.6%] 957–970 CE [12.8%] 973–994 CE [29.8%]	894–934 CE [35.2%] 940–995 CE [55.4%] 1006–1018 CE [4.8%]	100.0%	0% [*0%*]	899–920 CE [25.6%] 957–969 CE [12.4%] 972–994 CE [30.2%]	894–933 CE [35.2%] 940–996 CE [55.4%] 1006–1018 CE [4.8%]
AAR-29032	1099±27	898–922 CE [26.2%] 954–993 CE [42.0%]	891–995 CE [93.6%] 1007–1013 CE [1.8%]	100.0%	0% [*0%*]	898–922 CE [26.1%] 953–992 CE [42.1%]	891–995 CE [93.6%] 1007–1013 CE [1.8%]
AAR-29033	1071±29	901–918 CE [15.5%] 962–965 CE [1.7%] 975–997 CE [28.2%] 1002–1021 CE [22.7%]	895–929 CE [23.5%] 944–1026 CE [71.9%]	99.8%	0% [*0%*]	901–918 CE [15.7%] 962–965 CE [1.6%] 975–998 CE [28.4%] 1002–1021 CE [22.6%]	895–929 CE [23.5%] 944–1026 CE [71.9%]
AAR-29049	546±24	1330–1335 CE [6.4%] 1397–1423 CE [61.8%]	1325–1355 CE [27.2%] 1393–1429 CE [68.2%]	99.9%	0% [*0%*]	1330–1335 CE [6.9%] 1397–1423 CE [61.3%]	1324–1355 CE [27.3%] 1393–1429 CE [68.1%]
AAR-29050	591±23	1322–1358 CE [55.9%] 1391–1400 CE [12.3%]	1306–1365 CE [72.2%] 1384–1408 CE [23.2%]	99.9%	0% [*0%*]	1322–1357 CE [55.7%] 1391–1400 CE [12.5%]	1306–1365 CE [72.3%] 1384–1408 CE [23.1%]
AAR-29051	834±21	1181–1189 CE [8.7%] 1211–1232 CE [35.3%] 1241–1260 CE [24.2%]	1169–1171 CE [0.7%] 1175–1197 CE [17.0%] 1199–1265 CE [77.7%]	100.1%	0% [*0%*]	1181–1188 CE [8.5%] 1210–1233 CE [35.7%] 1241–1260 CE [24.0%]	1175–1197 CE [17.2%] 1198–1265 CE [78.2%]

Laboratory ID	^{14}C Age ^{14}C years BP	Calibrated age (68.2% conf.)	Calibrated age (95.4% conf.)	Model agreement	Outlier (posterior/ prior)	Calibrated age (posterior, 68.2% conf.)	Calibrated age (posterior, 95.4% conf.)
AAR-27638	1314±25	662–684 CE [29.3%]	657–706 CE [51.0%]	99.9%	0% [*0%*]	662–684 CE [29.5%]	657–706 CE [51.1%]
		699–704 CE [5.6%]	714–718 CE [1.2%]			699–704 CE [5.5%]	714–718 CE [1.2%]
		744–761 CE [24.2%]	726–732 CE [1.8%]			743–761 CE [24.3%]	726–731 CE [1.8%]
		766–773 CE [9.1%]	737–774 CE [41.4%]			766–773 CE [8.9%]	737–774 CE [41.3%]
AAR-27639	1262±25	681–748 CE [56.3%]	666–673 CE [1.8%]	99.8%	0% [*0%*]	681–748 CE [55.8%]	666–673 CE [1.8%]
		759–768 CE [5.9%]	677–775 CE [71.4%]			759–768 CE [5.9%]	677–775 CE [71.6%]
		772–775 CE [2.4%]	790–843 CE [19.2%]			772–775 CE [2.4%]	790–843 CE [19.1%]
		793–796 CE [1.4%]	856–866 CE [3.0%]			793–796 CE [1.7%]	857–866 CE [2.9%]
		834–838 CE [2.3%]				834–838 CE [2.3%]	
AAR-27625	1334±23	656–681 CE [49.6%]	652–693 CE [58.0%]	99.7%	0% [*0%*]	656–681 CE [49.1%]	652–693 CE [58.1%]
		750–759 CE [14.7%]	697–705 CE [5.5%]			749–759 CE [15.6%]	697–705 CE [5.5%]
		769–772 CE [3.9%]	742–773 CE [31.8%]			768–771 CE [3.6%]	742–773 CE [31.8%]
AAR-29009	1085±23	899–920 CE [24.8%]	894–932 CE [32.2%]	100.0%	0% [*0%*]	899–920 CE [24.7%]	894–931 CE [32.1%]
		957–969 CE [11.4%]	942–997 CE [54.1%]			957–969 CE [11.2%]	942–997 CE [54.3%]
		973–995 CE [32.0%]	1003–1021 CE [9.1%]			973–995 CE [32.3%]	1003–1021 CE [9.0%]
AAR-27620	1416±27	607–625 CE [35.1%]	599–659 CE [95.4%]	99.9%	0% [*0%*]	607–626 CE [35.2%]	599–659 CE [95.4%]
		637–653 CE [33.1%]				637–653 CE [33.0%]	
AAR-27617	1266±23	681–709 CE [23.3%]	665–775 CE [81.9%]	99.7%	0% [*0%*]	681–709 CE [23.3%]	665–775 CE [81.8%]
		711–746 CE [36.0%]	791–806 CE [4.1%]			711–746 CE [36.1%]	791–806 CE [4.1%]
		759–768 CE [6.6%]	810–824 CE [3.7%]			759–768 CE [6.4%]	810–824 CE [3.7%]
		772–775 CE [2.4%]	829–842 CE [4.2%]			772–775 CE [2.4%]	829–842 CE [4.2%]
			858–865 CE [1.6%]				858–865 CE [1.5%]
AAR-27619	1353±24	650–669 CE [57.6%]	644–686 CE [78.0%]	99.8%	0% [*0%*]	650–669 CE [57.5%]	644–686 CE [78.0%]
		671–678 CE [10.6%]	698–704 CE [2.3%]			671–678 CE [10.7%]	698–704 CE [2.3%]
			743–761 CE [11.7%]				743–762 CE [11.7%]
			765–773 CE [3.4%]				765–773 CE [3.4%]
AAR-29046	595±25	1320–1360 CE [55.3%]	1304–1367 CE [72.3%]	100.0%	0% [*0%*]	1320–1360 CE [55.5%]	1304–1367 CE [72.2%]
		1390–1399 CE [12.9%]	1382–1407 CE [23.1%]			1390–1399 CE [12.7%]	1382–1407 CE [23.2%]
AAR-29048	804±20	1225–1262 CE [68.2%]	1220–1270 CE [95.4%]	99.9%	0% [*0%*]	1225–1235 CE [19.7%]	1220–1270 CE [95.4%]
						1238–1261 CE [48.5%]	
AAR-29038	578±23	1325–1354 [50.5%]	1308–1363 [66.3%]	100.0%	0% [*0%*]	1325–1354 [50.6%]	1308–1363 [66.3%]
		1394–1404 [17.7%]	1388–1413 [29.1%]			1394–1404 [17.6%]	1388–1413 [29.1%]

Laboratory ID	^{14}C Age ^{14}C years BP	Calibrated age (68.2% conf.)	Calibrated age (95.4% conf.)	Model agreement	Outlier (posterior/ prior)	Calibrated age (posterior, 68.2% conf.)	Calibrated age (posterior, 95.4% conf.)
AAR-29039	842±23	1177–1194 [21.7%]	1166–1262 [95.4%]	99.9%	0% [*0%*]	1177–1194 [21.7%]	1166–1261 [95.4%]
		1201–1229 [39.3%]				1201–1229 [39.5%]	
		1247–1255 [7.1%]				1247–1254 [7.0%]	
AAR-27615	1412±33	606–627 [33.6%]	591–663 [95.4%]	99.9%	0% [*0%*]	607–627 [33.5%]	591–663 [95.4%]
		637–655 [34.6%]				637–655 [34.7%]	
AAR-27478	1309±27	663–685 [26.7%]	659–706 [47.8%]	99.9%	0% [*0%*]	663–685 [26.7%]	659–706 [47.7%]
		698–704 [6.4%]	714–718 [2.0%]			698–704 [6.3%]	714–718 [2.0%]
		743–763 [25.1%]	724–774 [45.6%]			743–763 [25.3%]	724–774 [45.7%]
		765–773 [10.0%]				765–773 [9.9%]	
AAR-29405	644±20	1300–1312 [20.1%]	1290–1325 [40.9%]	99.9%	0% [*0%*]	1300–1313 [22.3%]	1290–1325 [40.9%]
		1313–1318 [6.9%]	1355–1393 [54.5%]			1315–1318 [4.3%]	1355–1393 [54.5%]
		1361–1373 [20.2%]				1361–1373 [20.3%]	
		1376–1388 [21.0%]				1376–1388 [21.3%]	
AAR-29407	491±20	1422–1439 [68.2%]	1411–1445 [95.4%]	99.9%	0% [*0%*]	1422–1439 [68.2%]	1411–1445 [95.4%]

OxCal code

Here, the OxCal code for the entire age model is given. Outliers are not deleted from the code, but are kept as comments (with // or between /* and */), so their place in the stratigraphy can be seen. The probability distributions of the calibrated ages are coloured according to sample type, with charcoal samples being coloured dark grey (i.e., no "Color" command).

```
Options()
 {
  Resolution=1;
 };
 Plot()
 {
  Curve("AARHUS_curve.14c", "AARHUS_curve.14c");
  Outlier_Model("Charcoal",Exp(1,-10,0),U(0,3),"t");
  Sequence("Ribe")
  {
   Boundary("Start");
   Phase("Phase K01")
   {
    //    R_Date("AAR-29442 A973, P3161A birch charcoal", 2312, 25);
    //    R_Date("AAR-29443 A973, P3161B hazel charcoal", 2271, 24);
    R_Date("AAR-29444 A973, P3161C oak charcoal", 1420, 23)
    {
     Outlier("Charcoal",0.50);
    };
    //    R_Date("AAR-29445 A973, P3161D birch charcoal", 2297, 31);
   };
   Label("K02");
   Phase("Phase Post hole A996")
   {
    R_Date("AAR-29024 A996, P3157-1 birch charcoal", 1282, 23)
    {
     Outlier("Charcoal",0.05);
    };
    R_Date("AAR-29025 A996, P3157-2 birch charcoal", 1311, 25)
    {
     Outlier("Charcoal",0.05);
    };
    R_Date("AAR-29026 A996, P3157-3 birch charcoal", 1283, 24)
    {
     Outlier("Charcoal",0.05);
    };
    D_Sequence("A996 - 3 tree rings of a branch/little trunk")
    {
     R_Date("Innermost 1-2 year rings", 1283, 24);
     Gap(3);
     R_Date("Two year rings in the middle", 1311, 25);
     Gap(3);
     R_Date("Outermost two year rings", 1282, 23);
     Date("time of death A996");
    };
   };
   Phase("Phase Pit A970")
   {
    R_Date("AAR-29438 A970, P3121A elder charcoal", 1334, 28)
    {
     Outlier("Charcoal",0.50);
    };
    //    R_Date("AAR-29439 A970, P3121B birch charcoal", 1385, 26);
    R_Date("AAR-29440 A970, P3121C birch charcoal", 1303, 24)
    {
     Outlier("Charcoal",0.05);
    };
    R_Date("AAR-29441 A970, P3121D oak charcoal", 1317, 31)
    {
     Outlier("Charcoal",0.05);
    };
   };
   //phase pit A970
   Boundary("F3-F4");
   C_Date("Dendro F4 K5 grubehus A957 711-717",714,6);
   C_Date("Dendro F4 A932 716-727",722,10);
   Boundary("F4-F5");
   Phase("Phase F5 K12 House of the lyre")
   {
    Phase("Dendro 723/24")
    {
     C_Date("Dendro-date for house of the lyre A882 CE 723/724", 723.5,1);
    };
    Label("House A841, ash and dirt layer, A871");
    R_Date("AAR-29435 A871, X1310, P3000A hazel charcoal", 1253, 27)
    {
     Outlier("Charcoal",0.05);
    };
    R_Date("AAR-29436 A871, X1310, P3000B alder charcoal", 1290, 27)
    {
```

```
    Outlier(“Charcoal”,0.05);
   };
   R_Date(“AAR-29437 A871, X1310, P3000C alder charcoal”, 1214, 27)
   {
    Outlier(“Charcoal”,0.05);
   };
  };
  //phase f5 k12
  Boundary(“F5-F6”);
  Phase(“Phase F6, K15”)
  {
   D_Sequence(“A690 P2867 wiggle match”)
   {
    R_Date(“AAR-31325 year ring no. 1 (innermost)”, 1255, 33);
    Gap(20);
    R_Date(“AAR-31326 year ring no. 22 (outermost)”, 1296, 25);
    Date(“time of death A690 P2867”);
   };
  };
  C_Date(”Dendro A644 K15 eller K16 720-738”,729,18);
  Phase(“Phase F6, K16”)
  {
   R_Date(“AAR-29034 A590, X1227, P2906-1 rye grain”, 1284, 22)
   {
    Outlier(“Charcoal”,0.05);
   };
   //    R_Date(“AAR-29035 A590, X1227, P2906-2 alder charcoal”, 1387, 23);
   R_Date(“AAR-29036 A590, X1227, P2906-3 poplar charcoal”, 1247, 27)
   {
    Outlier(“Charcoal”,0.05);
   };
   C_Date(“Dendro A475 and A1111, P3162 and P3191, winter CE 733/34”,733.5,1);
  };
  //phase f6 k16
  Boundary(“F6-F7”);
  Phase(”Phase F7, K17”)
  {
   C_Date(”Dendro A612 K16 eller K17 vandretliggende CE 745/746”,745.5,2);
   //dendro A612 bræt, kasseret i K17’s brugstid
   C_Date(“Dendro A1123 K17 CE 726-741”,734,8);
   C_Date(“Dendro A1125 K17 CE 735-746”,741,6);
   C_Date(”K36 eller K17 F7 Dendro A497 CE 729-744”, 737, 16);
  };
  Phase(“Phase F7, K18”)
  {
/*    R_Date(“AAR-29432 A575, P2661A rye grain”, 1365, 26)
   {
    Outlier(“Charcoal”,0.05);
   };
   R_Date(“AAR-29433 A575, P2661B hulled barley grain”, 1204, 22)
   {
    Outlier(“Charcoal”,0.05);
   };
   R_Date(“AAR-29434 A575, P2661C hulled barley grain”, 1244, 22)
   {
    Outlier(“Charcoal”,0.05);
   };*/
  };
  Phase(“A443 K19”)
  {
   R_Date(“AAR-31398 A443 P2929 willow wood”, 1331, 25);
  };
  Phase(“A433”)
  {
   R_Date(“AAR-31324 hazel wood”, 1278, 26);
  };
  //phase F7 K18
/*   Phase(“Dendro 745-7”)
  {
   Label(“dendro-prøven mangler evt. splint”);
   C_Date(“Uppermost dendro-date between A440 and A396, CE 745-7”, 746, 2);
  };*/
  Boundary(“F7-F8”);
  Phase(“F8, K20 - Fireplace A403”)
  {
   R_Date(“AAR-29429 A403, X1002, P2553A oat grain”, 1312, 25)
   {
    Outlier(“Charcoal”,0.05);
   };
   R_Date(“AAR-29430 A403, X1002, P2553B charcoal cf sambucus”, 1311, 35)
   {
    Outlier(“Charcoal”,0.05);
   };
   R_Date(“AAR-29431 A403, X1002, P2553C alder charcoal”, 1303, 26)
   {
    Outlier(“Charcoal”,0.05);
   };
  };
  Boundary(“F8-F9”);
  Phase(“Phase A391 - the oldest wasp beads”)
  {
```

```
/*    R_Date("AAR-29021 A391, X953, P2507-1 hulled barley grain", 1184, 43)
    {
     Outlier("Charcoal",0.10);
    };*/
    R_Date("AAR-29022 A391, X953, P2507-2 rye grain", 1304, 23)
    {
     Outlier("Charcoal",0.10);
    };
    R_Date("AAR-29023 A391, X953, P2507-3 indet. grain", 1260, 25)
    {
     Outlier("Charcoal",0.10);
    };
   };
   Phase("Phase A351, construction")
   {
    D_Sequence("A351 - treerings, straw and wormhole")
    {
     R_Combine("treering no. 15 from the bark")
     {
      R_Date("treering no. 15 from the bark, 1st sample", 1320, 26);
      R_Date("treering no. 15 from the bark, 2nd sample", 1288, 26);
     };
     Gap(12);
     R_Date("third to last treering before bark", 1333, 28);
     Gap(1);
     R_Date("wormhole within the last treering", 1277, 24);
     //   Gap(1);
     R_Date("last treering before bark", 1312, 26);
     R_Date("straw from bark surface", 1307, 25);
     Date("time of Death3 A351");
    };
   };
   Phase("Phase A377")
   {
    R_Date("AAR-29043 A377, X938, P2498-1 hulled barley grain", 1283, 22)
    {
     Outlier("Charcoal",0.10);
    };
    //    R_Date("AAR-29044 A377, X938, P2498-2 hulled barley grain", 833, 21);
    R_Date("AAR-29045 A377, X938, P2498-3 indet. grain", 1262, 31)
    {
     Outlier("Charcoal",0.10);
    };
   };
   D_Sequence("A363 - 3 tree rings of a branch")
   {
    R_Date("treering no. 7 from the bark", 1305, 22);
    Gap(2);
    R_Date("treering no. 4 from the bark", 1270, 24);
    Gap(2);
/*    R_Combine("outermost treering (2 dates)")
       {
      R_Date("outermost treering, 1st sample", 1335, 15);
      R_Date("outermost treering, 2nd sample", 1363, 25);
   }; */
    Date("time of death A363");
   };
   Phase("Phase A362")
   {
    R_Date("AAR-29015 A362, X892, P2457-1 oat grain", 1274, 30)
    {
     Outlier("Charcoal",0.10);
    };
    R_Date("AAR-29016 A362, X892, P2457-2 poplar charcoal", 1295, 22)
    {
     Outlier("Charcoal",0.10);
    };
    R_Date("AAR-29017 A362, X892, P2457-3 alder charcoal", 1246, 25)
    {
     Outlier("Charcoal",0.10);
    };
   };
   Phase("Phase 9d")
   {
    R_Date("AAR-29426 P2438A A354 poplar charcoal", 1163, 31)
    {
     Outlier("Charcoal",0.10);
    };
    R_Date("AAR-29427 P2438B A354 alder/birch charcoal", 1334, 26)
    {
     Outlier("Charcoal",0.10);
    };
    //    R_Date("AAR-29428 P2438C A354 alder charcoal", 1508, 33);
    R_Date("AAR-32115 A357 P2445 X875 hazel nutshell", 1260, 22)
    {
     Outlier("Charcoal",0.05);
    };
    Interval( "Duration of phase 9d");
   };
   Phase("Phase A351, use/destruction")
   {
```

```
    R_Date("AAR-29423 P2428A A351 alder charcoal", 1204, 21)
    {
     Outlier("Charcoal",0.10);
    };
    R_Date("AAR-29424 P2428B A351 alder charcoal", 1196, 22)
    {
     Outlier("Charcoal",0.10);
    };
    R_Date("AAR-29425 P2428C A351 willow charcoal", 1165, 26)
    {
     Outlier("Charcoal",0.10);
    };
    R_Date("AAR-30137 A351 indet. charcoal", 1240, 16)
    {
     Outlier("Charcoal",0.50);
    };
   };
   Phase("Phase A350")
   {
    R_Date("AAR-29420 P2425A A350 barley grain", 1234, 24)
    {
     Outlier("Charcoal",0.10);
    };
/*    R_Date("AAR-29421 P2425B A350 barley grain", 595, 21);
       R_Date("AAR-29422 P2425C A350 indet. grain", 784, 23); */
   };
   Phase("Phase 9f")
   {
    R_Date("AAR-32114 A348 P2382B rye grain", 1242, 28)
    {
     Outlier("Charcoal",0.05);
    };
   };
   Boundary("F9-F10");
   Phase("A316")
   {
    //     R_Date("AAR-29414 P2363A A316 rye grain", 871, 23);
    R_Date("AAR-29415 P2363B A316 rye grain", 1259, 23)
    {
     Outlier("Charcoal",0.50);
    };
    R_Date("AAR-29416 P2363C A316 hazel charcoal", 1217, 22)
    {
     Outlier("Charcoal",0.05);
    };
   };
   Phase("A320")
   {
    R_Date("AAR-29018 A320, P2358-1 alder charcoal", 1228, 21)
    {
     Outlier("Charcoal",0.05);
    };
    R_Date("AAR-29019 A320, P2358-2 hazel charcoal", 1184, 22)
    {
     Outlier("Charcoal",0.05);
    };
    R_Date("AAR-29020 A320, P2358-3 hazel charcoal", 1261, 24)
    {
     Outlier("Charcoal",0.05);
    };
   };
   R_Date("AAR-30136 A294 Nutshell (hassel)", 1243, 15)
   {
    Outlier("Charcoal",0.05);
   };
   Phase("Floor horizon E, lower, A288")
   {
/*    R_Date("AAR-29027 A288 uncertain context, X665, P2296-1 oat grain", 745, 26);
        R_Date("AAR-29028 A288 uncertain context, X665, P2296-2 hulled barley grain", 289, 31);
        R_Date("AAR-29029 A288 uncertain context, X665, P2296-3 deciduous tree charcoal", 842, 22); */
    R_Date("AAR-29411 P2297A A288 alder charcoal", 1185, 19)
    {
     Outlier("Charcoal",0.05);
    };
    R_Date("AAR-29412 P2297B A288 alder charcoal", 1199, 25)
    {
     Outlier("Charcoal",0.05);
    };
    R_Date("AAR-29413 P2297C A288 poplar/willow charcoal", 1189, 20)
    {
     Outlier("Charcoal",0.05);
    };
   };
   //phase A288
   //   Boundary("Shift to small cut beads");
   Phase("Average Floor horizon E, upper, dirt layer, A263")
   {
/*    R_Date("AAR-29052 A263, P2281-1 birch charcoal", 1158, 23)
    {
     Outlier("Charcoal",0.05);
    };*/
```

```
    R_Date("AAR-29053 A263, P2281-2 alder charcoal", 1191, 22)
    {
     Outlier("Charcoal",0.05);
    };
    R_Date("AAR-29054 A263, P2281-3 poplar charcoal", 1232, 21)
    {
     Outlier("Charcoal",0.05);
    };
   };
   Boundary("F10-F11");
   Phase("Phase K23")
   {
    R_Date("AAR-27643 A239 X453A Cattle", 1255, 25)
    {
     Outlier("Charcoal",0.50);
    };
    R_Date("AAR-29056 A239, P667-1 barley grain", 1208, 30)
    {
     Outlier("Charcoal",0.05);
    };
    R_Date("AAR-29057 A239, P667-2 rye grain", 1186, 29)
    {
     Outlier("Charcoal",0.05);
    };
    //    R_Date("AAR-29058 A239, P667-3 rye grain", 527, 22);
   };
   Boundary("F11-F12");
   Phase("Phase F12")
   {
    Sequence("Sequence K24 - K25")
    {
     Phase("Phase A225")
     {
      R_Date("AAR-29408 A225 parcel 1 x414 P654A barley grain", 1218, 22)
      {
       Outlier("Charcoal",0.05);
      };
      R_Date("AAR-29409 A225 parcel 1 x414 P654B oat grain", 1172, 25)
      {
       Outlier("Charcoal",0.05);
      };
      //    R_Date("AAR-29410 A225 parcel 1 x414 P654C rye grain", 380, 24);
     };
/*   Phase("Phase A230")
   {
    R_Date("AAR-29031 A230, P651-1 wheat grain", 1090, 23);
    R_Date("AAR-29032 A230, P651-2 rye grain", 1099, 27);
    R_Date("AAR-29033 A230, P651-3 rye grain", 1071, 29);
   };*/
     Label("K25");
     Phase("Phase A11")
     {
      R_Date("AAR-27640 A11 X352A Cattle", 1231, 32)
      {
       Outlier("Charcoal",0.05);
      };
/*    R_Date("AAR-29049 P617-1, A11, lag 5 birch charcoal", 546, 24);
          R_Date("AAR-29050 P617-2, A11, lag 5 birch charcoal", 591, 23);
          R_Date("AAR-29051 P617-3, A11, lag 5 charcoal (Pomoideae)", 834, 21);  */
     };
     Phase("Phase A165 and A196")
     {
      //    R_Date("AAR-27638 A196 x310A Cattle", 1314, 25);
      R_Date("AAR-27634 A165 x323A Cattle", 1188, 27)
      {
       Outlier("Charcoal",0.05);
      };
     };
     //phase A165 and A196
    };
    //sequence K24-K25
    R_Date("AAR-27633 A159 x227A Cattle", 1208, 25)
    {
     Outlier("Charcoal",0.05);
    };
/*    R_Date("AAR-27639 A198 X326A Cattle", 1262, 25)*/
    R_Date("AAR-27642 A216 X379A Cattle", 1213, 35)
    {
    Outlier("Charcoal",0.05);
    };
   };
   //phase f12
   Boundary("F12-F13");
   Phase("F13")
   {
    Label("K26");
    R_Date("AAR-27629 A135 X179A Cattle", 1201, 24)
    {
     Outlier("Charcoal",0.05);
    };
    Phase("A127")
```

```
 {
  //     R_Date("AAR-27625 A127 x160A Burnt bone", 1334, 23);
  //     R_Date("AAR-29009 A127, P246-1 oat grain", 1085, 23);
  R_Date("AAR-29010 A127, P246-2 rye grain", 1216, 27)
  {
   Outlier("Charcoal",0.05);
  };
  R_Date("AAR-29011 A127, P246-3 birch charcoal", 1194, 24)
  {
   Outlier("Charcoal",0.05);
  };
 };
 Phase("A114")
 {
  R_Date("AAR-27622 A114 X146B Red deer antler", 1196, 28)
  {
   Outlier("Charcoal",0.05);
  };
  R_Date("AAR-27621 A114 X146A Red deer antler", 1191, 24)
  {
   Outlier("Charcoal",0.05);
  };
 };
 Phase("A101")
 {
  R_Date("AAR-29012 P169-1, A101 birch charcoal", 1184, 22)
  {
   Outlier("Charcoal",0.05);
  };
  R_Date("AAR-29013 P169-2, A101 hazel charcoal", 1178, 24)
  {
   Outlier("Charcoal",0.05);
  };
  R_Date("AAR-29014 P169-3, A101 alder charcoal", 1223, 22)
  {
   Outlier("Charcoal",0.05);
  };
 };
};
//phase f13
//    R_Date("AAR-27620 A110 X121A Red deer antler", 1416, 27);
Boundary("F13-F14");
Phase("F14")
{
 Label("K27");
 Phase("Phase A96")
 {
  D_Sequence("P198, A96 wiggle match")
  {
   R_Date("AAR-29403 P198 ring 4", 1179, 26);
   Gap(17);
   R_Date("AAR-29404 P198 ring 22", 1217, 21);
   Date("time of death P198 A96");
  };
  //    R_Date("AAR-27617 A96 X104A Red deer antler", 1266, 23);
  R_Date("AAR-31323 A96 alder charcoal", 1173, 25);
 };
 Phase("Phase A94 and A98")
 {
  R_Date("AAR-29006 X130, A94, P570-1 rye grain", 1151, 26)
  {
   Outlier("Charcoal",0.05);
  };
  R_Date("AAR-29007 X130, A94, P570-2 rye grain", 1111, 24)
  {
   Outlier("Charcoal",0.05);
  };
  R_Date("AAR-29008 X130, A94, P570-3 rye grain", 1117, 24)
  {
   Outlier("Charcoal",0.05);
  };
  //    R_Date("AAR-27619 A98 X108B Red deer antler", 1353, 24);
  R_Date("AAR-27618 A98 X108A Cattle decid. tooth", 1134, 24)
  {
   Outlier("Charcoal",0.05);
  };
  //    R_Date("AAR-29046 A98, P201-1 rye grain", 595, 25);
  R_Date("AAR-29047 A98, P201-2 rye grain", 1088, 22)
  {
   Outlier("Charcoal",0.05);
  };
  //    R_Date("AAR-29048 A98, P201-3 rye grain", 804, 20);
  R_Date("AAR-30135 A98 Charcoal (el/hassel)", 1124, 15)
  {
   Outlier("Charcoal",0.05);
  };
 };
 R_Date("AAR-30134 A93 Charred nut shell (hassel)", 1113, 17)
 {
  Outlier("Charcoal",0.05);
 };
```

```
    Phase(“A86”)
    {
     // R_Date(“AAR-29038 A86, X91, P196-1 hulled barley grain”, 578, 23);
     // R_Date(“AAR-29039 A86, X91, P196-2 oat grain”, 842, 23);
     R_Date(“AAR-29040 A86, X91, P196-3 rye grain”, 1111, 24)
     {
      Outlier(“Charcoal”,0.05);
     };
/*    R_Date(“AAR-27615 A86 X93A Red deer antler”, 1412, 33)*/
    };
   };
   //phase f14
   Boundary(“End”);
  };
  //sequence
  Sequence(“Plot 2”)
  {
   Boundary(“StartPlot2”);
   C_Date(“F9 Dendro A387 CE 745-760”, 753, 16);
   Boundary(“F12-F13_Plot2”);
   Label(“K31”);
   R_Date(“AAR-27637 A194 x304A Burnt bone”, 1279, 22)
   {
    Outlier(0.5);
   };
   Phase(“Phase A178”)
   {
    R_Date(“AAR-27635 A178 x276A Cattle”, 1319, 23)
    {
     Outlier(0.5);
    };
    R_Date(“AAR-27636 A178 x276B Cattle”, 1264, 24)
    {
     Outlier(0.5);
    };
    R_Date(“AAR-29055 P395 A178 Hazel charcoal”, 1209, 20)
    {
     Outlier(0.5);
    };
    D_Sequence(“P395, A178, X276 - two samples of alder charcoal”)
    {
     R_Date(“AAR-29042 inner sample”, 1245, 26)
     {
      Outlier(0.5);
     };
     Gap(27);
     R_Date(“AAR-29041 outer sample”, 1206, 21)
     {
      Outlier(0.5);
     };
     Date(“time of death A178”);
    };
    //dsequence
   };
   Phase(“Phase A158”)
   {
    R_Date(“AAR-27632 A158 x224B Sheep/goat”, 1235, 28)
    {
     Outlier(0.5);
    };
    R_Date(“AAR-27631 A158 x224A Cattle”, 1234, 22)
    {
     Outlier(0.5);
    };
   };
   R_Date(“AAR-27630 A152 x209A Cattle”, 1240, 25)
   {
    Outlier(0.5);
   };
   Phase(“Phase A130”)
   {
    R_Date(“AAR-27627 A130 x197A Cattle”, 1332, 24)
    {
     Outlier(0.5);
    };
    R_Date(“AAR-27628 A130 x197B Red deer antler”, 1201, 23)
    {
     Outlier(0.5);
    };
   };
   Boundary(“F13-F14_plot2”);
   Phase(“A124”)
   {
/*    R_Date(“AAR-27478 A124 X165 Red deer antler”, 1309, 27)
    R_Date(“AAR-29405 P234A dirt layer between clay layers of A124, rye grain”, 644, 20);*/
    R_Date(“AAR-29406 P234B dirt layer between clay layers of A124, alder/birch charcoal”, 1227, 22);
    //  R_Date(“AAR-29407 P243C dirt layer between clay layers of A124, beech charcoal”, 491, 20);
   };
   Boundary(“EndPlot2”);
  };
  //sequence plot2
```

```
  Difference("Difference1","F12-F13","F12-F13_Plot2",N(0,20));
  Difference("Difference2","F13-F14","F13-F14_plot2",N(0,20));
  Difference("Difference3","End","EndPlot2",N(0,20));
  Label("Outliers");
  R_Date("AAR-29442 A973, P3161A birch charcoal", 2312, 25);
  R_Date("AAR-29443 A973, P3161B hazel charcoal", 2271, 24);
  R_Date("AAR-29445 A973, P3161D birch charcoal", 2297, 31);
  R_Date("AAR-29439 A970, P3121B birch charcoal", 1385, 26);
  R_Date("AAR-29035 A590, X1227, P2906-2 alder charcoal", 1387, 23);
  R_Date("AAR-29432 A575, P2661A rye grain", 1365, 26);
  R_Date("AAR-29021 A391, X953, P2507-1 hulled barley grain", 1184, 43);
  R_Date("AAR-29044 A377, X938, P2498-2 hulled barley grain", 833, 21);
  R_Combine("outermost treering (2 dates)")
  {
   R_Date("outermost treering, 1st sample", 1335, 15);
   R_Date("outermost treering, 2nd sample", 1363, 25);
  };
  R_Date("AAR-29428 P2438C A354 alder charcoal", 1508, 33);
  R_Date("AAR-29421 P2425B A350 barley grain", 595, 21);
  R_Date("AAR-29422 P2425C A350 indet. grain", 784, 23)}
  R_Date("AAR-29027 A288 uncert. cont., X665, P2296-1 oat grain", 745, 26);
  R_Date("AAR-29028 A288 uncert. cont., X665, P2296-2 hulled barley grain", 289, 31);
  R_Date("AAR-29029 A288 uncert. cont., X665, P2296-3 deciduous tree charcoal", 842, 22);
  R_Date("AAR-29058 A239, P667-3 rye grain", 527, 22);
  R_Date("AAR-29410 A225 parcel 1 x414 P654C rye grain", 380, 24);
  R_Date("AAR-29031 A230, P651-1 wheat grain", 1090, 23);
  R_Date("AAR-29032 A230, P651-2 rye grain", 1099, 27);
  R_Date("AAR-29033 A230, P651-3 rye grain", 1071, 29);
  R_Date("AAR-29049 P617-1, A11, lag 5 birch charcoal", 546, 24);
  R_Date("AAR-29050 P617-2, A11, lag 5 birch charcoal", 591, 23);
  R_Date("AAR-29051 P617-3, A11, lag 5 charcoal (Pomoideae)", 834, 21);
  R_Date("AAR-27638 A196 x310A Cattle", 1314, 25);
  R_Date("AAR-27639 A198 X326A Cattle", 1262, 25);
  R_Date("AAR-27625 A127 x160A Burnt bone", 1334, 23);
  R_Date("AAR-29009 A127, P246-1 oat grain", 1085, 23);
  R_Date("AAR-27620 A110 X121A Red deer antler", 1416, 27);
  R_Date("AAR-27617 A96 X104A Red deer antler", 1266, 23);
  R_Date("AAR-27619 A98 X108B Red deer antler", 1353, 24);
  R_Date("AAR-29046 A98, P201-1 rye grain", 595, 25);
  R_Date("AAR-29048 A98, P201-3 rye grain", 804, 20);
  R_Date("AAR-29038 A86, X91, P196-1 hulled barley grain", 578, 23);
  R_Date("AAR-29039 A86, X91, P196-2 oat grain", 842, 23);
  R_Date("AAR-27615 A86 X93A Red deer antler", 1412, 33);
  R_Date("AAR-27478 A124 X165 Red deer antler", 1309, 27);
  R_Date("AAR-29405 P234A dirt layer between clay layers of A124, rye grain", 644, 20);
  R_Date("AAR-29407 P243C dirt layer between clay layers of A124, beech charcoal", 491, 20);
 };
```

Supplementary References

(References 1-44 are in the main text, references 45-58 are with the Methods section (online only))

59. Skre, D. 2008. Post-substantivist Towns and Trade CE 600-1000. In: D. Skre (ed.) *The Means of Exchange. Kaupang Excavation Projekt Publication Series, 2*. Aarhus: Aarhus University Press, 327-341.

60. Kleingärtner S. 2014. Die frühe Phase der Urbanisierung an der südlichen Ostseeküste im ersten nachchristlichen Jahrtausend. Studien zur Siedlungsgeschichte und Archäologie der Ostseegebiete 13. Neumünster: Wachholtz.

61. Sindbæk, S.M. 2017. Urbanism and exchange in the North Atlantic/Baltic, 600-1000 CE. In T. Hodos (ed.), *The Routledge Handbook of Archaeology and Globalization*. New York etc.: Routledge, 553-565.

62. Feveile, C. 2006. Ribe on the north side of the river, 8th-12th century. In: C. Feveile (ed.) Det ældste Ribe. Udgravninger på nordsiden af Ribe Å 1984-2000. Ribe Studier bd 1.1. Aarhus: Jysk Arkæologisk Selskab, 65-92.

63. Feveile, C. 2012. Ribe: Emporia and Town in 8th–9th Century. In: S. Gelichi & R. Hodges (ed.), *From One Sea to Another: Tring Places in the European and Mediterranean Early Middle Ages*. Turnhout: Brepols, 111–22.

64. Feveile, C. & S. Jensen 2000. Ribe in the 8th and 9th century. A Contribution to the Archaeological Chronology of North Western Europe. Acta Archaeologica 71, 9–24.

65. Feveile, C. & Jensen, S. 2006. ASR 9 Posthuset. In: C. Feveile (ed.) Ribe Studier. Det Ældste Ribe. Ud-

gravninger på nordsiden af Ribe Å 1984–2000. Bind 1.2. Højbjerg: Jysk Arkæologisk Selskab, pp. 119–89.

66. Brinch Madsen, H. 1984. Metal-casting, techniques, production and workshops, in M. Bencard (ed.) *Ribe excavations 1970–1976. Volume* 2: 15-189. Esbjerg: Sydjysk Universitetsforlag.

67. Jansson, I., 1985. *Ovala spännbucklor: en studie av vikingatida standardsmycken med utgångspunkt från Björkö-fynden*. I. Jansson.

68. Klæsøe, I.S., 1999. Vikingetidens kronologi – en nybearbejdning af det arkæologiske materiale. *Aarbøger for Nordisk Oldkyndighed og Historie*, (1997), pp.89-142.

69. Callmer, J. 1991. Beads as a criterion of shifting tre and exchange connections. *Studien zur Sachsenforschung* 7, 1991: 25 38.

70. Šmit, Ž., Knific, T., Jezeršek, D. and Istenič, J., 2012. Analysis of early medieval glass beads – Glass in the transition period. *Nuclear Instruments and Methods in Physics Research Section B: Beam Interactions with Materials and Atoms*, *278*, pp.8-14.

72. Astrup, E.E. and Andersen, A.G., 1987. A study of metal foiled glass beads from the Viking period. *Acta archaeologica*, *58*, pp.222-228.

73. Feveile, C., Sode, T. and Schnell, U., 2010. An investigation on segmented, metal-foiled glass beads and blown, mirrored glass beads from Ribe, Denmark. In *Zwischen Fjorden und Steppe* (pp. 319-328).

74. Andrae, R., 1975. Mosaikaugenperlen: Untersuchungen zur Verbreitung und Datierung karolingerzeitlicher Millefioriglasperlen in Europa. Acta Praehistorica et Archaeologica 4 (1973): 101-198

75. Pöche, A., 2002. *Die Glasfunde des frühmittelalterlichen Handelsplatzes von Groß-Strömkendorf bei Wismar* (Doctoral dissertation, Christian-Albrechts-Universiät, Kiel).

76. Ambrosiani, B., 2013. *Stratigraphy: Part One: the Site and the Shore, Part Two: the Bronze Caster's Workshop*. Birka Project, Riksantikvarieämbetet.

77. Sanke, M. 2001. Gelbe Irdenware. I: H. Lüdtke & K. Schietzel (ed.): *Handbuch zur mittelalterlichen Keramik in Nordeuropa*. bd. 1. 271-428.

78. Stilke, H. 2001: Tatinger Ware. In: H. Lüdtke & K. Schietzel (ed.): *Handbuch zur mittelalterlichen Keramik in Nordeuropa*. bd. 1. 257-270.

79. Schön, V. 1995. *Die Mühlsteine von Haithabu und Schleswig.* Berichte über die Ausgrabungen in Haithabu 31. Neumünster (Karl Wachholtz Verlag).

80. Feveile, C., 2010. Mayen Basalt from the Ribe Excavations 1970-76. In *Jysk Arkæologisk Selskabs Skrifter* (pp. 133-156). Jysk Arkæologisk Selskab.

81. Baug, I., 2017. Soapstone vessels and quernstones as commodities in the Viking Age and Middle Ages. In *Viking-Age Transformations* (pp. 139-159). Routledge.

82. Feveile, C., 2008. Series X and coin circulation in Ribe. Studies in Early Medieval Coinage 1, 53–67.

83. Tyers, I.G. 1997. Dendro for Windows Program Guide. ARCUS Report 340. Sheffield.

84. Hollstein, E. 1980. Mitteleuropäische Eichenchronologie. Trierer dendrochronologische Forschungen zur Archäologie und Kunstgeschichte. Mainz am Rhein, Verlag Philipp von Zabern.

85. Usoskin, I. G., Kromer, B., Ludlow, F. ,Beer, J., Friedrich, M., Kovaltsov, G. A., Solanki, S. K. and Wacker, L. 2013. The AD775 cosmic event revisited: the Sun is to blame. Astronomy & Astrophysics 552.

86. Jull, A. J. T., Panyushkina, I. P., Lange, T. E., Kukarskih, V. V., Myglan, V. S.,Clark, K. J., Salzer, M. W., Burr, G. S. and Leavitt, S. W. 2014. Excursions in the 14C record at A.D. 774–775 in tree rings from Russia and America. Geophysical Research Letters 41(8): 3004-3010.

87. Rakowski, A. Z., Krapiec, M., Huels, M., Pawlyta, J., Dreves, A. and Meadows, J. 2015. Increase of radiocarbon concentration in tree rings from Kujawy (SE Poland) around AD 774-775. Nuclear Instruments & Methods in Physics Research Section B-Beam Interactions with Materials and Atoms 361: 564-568.

88. Oppenheimer, C., Wacker, L., Xu, J., Galván, J. D., Stoffel, M., Guillet, S., Corona, C., Sigl, M., Di Cosmo, N., Hajdas, I., Pan, B., Breuker, R., Schneider, L., Esper, J., Fei, J., Hammond, J. O. S. and Büntgen, U. 2017. Multi-proxy dating the 'Millennium Eruption' of Changbaishan to late 946 CE. Quaternary Science Reviews 158: 164-171.

Acknowledgments: We would like to thank the excavators of the site, whose work formed the basis for this study: Henrik Brinch Christiansen, Maria Knudsen, Sarah Qvistgaard and Morten Søvsø from Museum of Southwest Jutland, and Sarah Croix and Pieterjan Deckers from Aarhus University. The large numbers of radiocarbon dates would not have been possible without the support of the staff and PhD students of the Aarhus AMS Centre: Alexandra Fogtmann-Schulz, Claus Grosen, Hanne Jakobsen, Marie Kanstrup, Sabrina Gjødvad Kaiser Kudsk, Mette Sand Kalaee and Ann Berith Valbøl Jensen.

Funding: This study was funded by the Carlsberg Foundation Semper Ardens Grant CF16-0008 (Northern Emporium project) and the Danish National Research Foundation grant DNRF119 – Centre of Excellence for Urban Network Evolutions (UrbNet). Brødrene Hartmanns Fond (grant application A34514) and Grosserer P.L. Jørgensens Mindefond supported the tree-rings measurements with 50.000 DKK and 25.000 DKK, respectively.

Author contributions: Conceptualization: JO, SMS; Data curation: BP, CF, JO, SMS; Formal Analysis BP, JO; Funding acquisition SMS, JO, BP; Investigation BP, CF, JO, SMS; Methodology BP, CF, JO, SMS; Project administration SMS, CF; Visualization BP, JO; Writing – original draft: BP, SMS, JO; Writing – review & editing: BP, CF.

Competing interests: The authors declare no competing interests.

Data and materials availability: All data and code is available in the main text or the Supplementary Information. Additional information about the site and excavation can be found at https://projects.au.dk/northernemporium/, additional artefact photographs at http://sol.sydvestjyskemuseer.dk/ using the search term ”SJM 3 ”.